DETERMINISTIC MODELING OF SUSPENDED SEDIMENT LOAD IN THE UPPER ATHI RIVER CATCHMENT

BY

ODHIAMBO, TOMKIN ODO

Bsc Hons (Agric. Eng), Egerton University

This thesis is submitted to the University of Nairobi in partial fulfillment of the requirements for the degree of Masters of Science

IN

ENVIROMENTAL AND BIOSYSTEM ENGINEERING
(SOIL AND WATER ENGINEERING)

DEPARTMENT OF ENVIROMENTAL AND BIOSYSTEM ENGINEERING
FACULTY OF ENGINEERING
UNIVERSITY OF NAIROBI

May 2005

DECLARATION

CANDIDATE

This thesis is my original work and has not been presented for a degree in any other university. No part of this thesis may be reproduced without the prior permission of the University of Nairobi

Signed............................Date July 18, 2005

Odhiambo Tomkin Odo

Registration No: F56/7648/2000

SUPERVISOR

This thesis has been submitted with my approval as the university supervisor

Signed..............................Date 19 July 2005

Name: Albert Kenyani Inima

Lecturer, Department of Environmental and Biosystem Engineering

DEDICATION

To my parents Mr. and Mrs. Odo; to my wife Ruth and my daughter Liz, whose sacrifices, commitments and encouragement in seeing me through my education is something I will always remember and which will continue being a source of inspiration

ABSTRACT

TITLE: DETERMINISTIC MODELLING OF SUSPENDED SEDIMENT LOAD IN THE UPPER ATHI RIVER CATCHMENT

AUTHOR: ODHIAMBO TOMKIN ODO

The study is based on the upper Athi River sub-catchment, which comprises an area of approximately 5 590 km^2 and is bounded by the parallels of latitude 0 ^{0} 50 ' S and 1 ^{0} 50 ' S, and the meridians 36 ^{0} 30 ' E and 37 ^{0} 15 ' E. There are two high points making the sub-catchment. That is, the southern slope of the Aberdare ranges together with the flanks of the rift valley to the south and Ngong hills, which is to the west.

Sediments, which are by-products of runoff, reduce soil fertility and the economic life of reservoirs. In the Athi river catchment, sediment transport estimates from 1965 and earlier indicate that this catchment lost 55 000 tonnes of sediment annually. Tana and Athi River Development Authority (TARDA) carried some work on the river in 1983 and noted that this figure is increasing annually. With this increase, the following sediment problems are experienced in the catchment; reduction in reservoir life due to sedimentation, turbine operation being adversely affected, water pumps are adversely affected, intake structures and irrigation canals have silted up and river channel sediment deposition clogs the rivers causing floods during rainy seasons and shortage of water during dry seasons. This results in fish production being drastically reduced while the deposition of fine sediment at the river mouth results in mud floods. These mud floods are colonized by mangrove vegetation. Malindi Beach has been extended in the last 20 years as a result of this deposition. For much of the year, the water of the beach is too loaded with fine silt, making it less attractive for beach tourism.

The above problems call for sediment studies in the catchment. The present study is based on suspended sediment load using rainfall, runoff and suspended sediment

data obtained during the period 1980 to 1981. All the data used were first subjected to statistical tests in order to verify their homogeneity and validity. Forecasting the suspended sediment yield during the period of study was done using the Instantaneous Unit Sediment Graph (IUSG) model, which is a conceptual multi-reservoir cascading system that was developed by Professor Nash in 1957. The IUSG model was changed to T hr USG using the convolution integral method. A sediment rating equation was also developed using the ordinary least squares method. A rating equation was obtained by considering the log-normal distribution of the error component, which represents the state-of-the-art in rating equations.

For the period of the study, the total estimated sediment yield from the sub-catchment was obtained as 1.05 million tonnes compared to 660 000 tonnes by Wain in 1983. This translates to one eighth of the sediment yield from the entire catchment monitored at Sabaki River by Mansell-Muollin in 1973. The mean rate of sediment production was obtained as 187.95 t/km^2 /yr, which is high compared to 118 t/km^2 /yr obtained by Wain in 1983. Wain used the flow duration-sediment rating curve, which is known to be inaccurate when compared to the IUSG model.

Due to lack of resources, the catchment was not gauged for present runoff and sediment data. Therefore, the forecasted sediment yield does not reflect the present status of sediment yield in the catchment. It is, therefore, recommended that the catchment be gauged for up to date runoff and sediment discharge data, as the catchment has undergone various land use changes that have increased the sediment yield, thus compounding the sediment problems discussed above.

TABLE OF CONTENTS

LIST OF TABLES

LIST OF FIGURES

LIST OF ABBREVIATIONS

ASSS:	Automatic Single Stage Sampling
DRD:	Direct Rainfall Depth
DRH:	Direct Runoff Hydrograph
DRUH:	Direct Runoff Unit Hydrograph
DWHM:	Digital Watershed Hydrologic Modelling
EAAFRO:	East Africa Agricultural and Forestry Organization
EDI:	Equal Discharge Interval Instantaneous Unit Graph
EE:	Empirical Equations
ERH:	Excess Rainfall Hydrograph
ETR:	Equal Transit Rate
GS:	Grab Sampling
IUH:	Instantaneous Unit Hydrograph
IUSG:	Instantaneous Unit Sediment Graph
LST:	Linear System Theory
ML_1:	1st Moment of Area of the ERH about the Origin
ML_2:	2nd Moment of Area of the ERH about the Origin
MUSLE:	Modified Universal Soil Loss Equation
MQ_1:	1st Moment of Area of the DRH about the Origin
MQ_2:	2nd Moment of Area of the DRH about the Origin
OLS:	Ordinary Least Squares
PH:	Potential of Hydrogen
RC:	Routing Concepts
RCP:	Representative Catchment Project
SA:	Stochastic Approaches
SDR:	Sediment Delivery Ratio
SRC:	Sediment Rating Curve
TARDA:	Tana and Athi River Development Authority
TUH:	T-hour Unit Hydrograph

TUSG: T-hour Unit Sediment Graph

USG: Unit Sediment Graph

UH: Unit Hydrograph

ACKNOWLEDGEMENT

The author gratefully acknowledges the help received from Mr. A.K. Inima for his tireless efforts in providing support and supervision of this study, and to the entire staff of the Department of Environmental and Biosystem Engineering, University of Nairobi, for their support at varying stages of the work.

Special appreciation also goes to my friends, brothers and colleagues who contributed in many ways through frequent contacts. The assistance provided by the University of Nairobi by financing the study is also specially acknowledged. The Ministry of Water Development and the Kenya Meteorological Department, Kenya, is also appreciated for providing the data used in this study. It is not possible to mention everybody who contributed in this study, but to all I say thank you.

1.0 CHAPTER ONE: INTRODUCTION

1.1 BACKGROUND

The Athi River, also known as the Galana and the Sabaki in its lower reaches, constitutes one of the most important surface water resources in Kenya. The river supports many small-scale irrigation schemes that are mostly found in the upper reaches. It also supplies water to various rural water schemes. Mombasa and Nairobi towns obtain 83% and 16% (respectively) of their water from the river (TARDA, 1981). A rapid increase in population of the Catchment of the Athi River has caused a corresponding decrease in the plant cover that has resulted in an increased sediment runoff. This study developed a model that was used to estimate the sediment runoff in the upper reach of this Catchment. The data that was used for the development of the model was obtained from the Ministry of Water Development. The Instantaneous Unit Sediment Graph (IUSG) Model was applied to these data for the period 1980 to 1981.The data available covers this period.

The IUSG is defined as the distribution of sediment that arises from an instantaneous burst of rainfall producing one unit of mobilized sediment (Kumar and Rastogi, 1987). The IUSG is similar to the Instantaneous Unit Hydrograph (IUH), which is the time distribution of direct runoff that would be caused by a unit of excess rainfall falling onto the Catchment instantaneously. The IUSG was analyzed using the concept of a multi-reservoir cascading system as developed by Nash in 1957 and that is well documented (Chow et al, 1988). In this conceptual model, the fluvial system is desegregated into an integer number of linear reservoirs (say n). An inflow unit mass of sediment is routed through each of these reservoirs to obtain the sediment at the sediment metering station. An optimization technique was used to determine the model parameters that best forecast the measured sediment.

1.2 THE STUDY AREA

We have five major catchments in Kenya. The Upper Athi River subcatchment falls under catchment area number three, which comprises of areas on the southern slopes of the Aberdare ranges and the flanks of the Rift Valley all the way to the southern part to form the Athi River. At the lower reaches, it is joined by Tsavo River and becomes known as the Sabaki River. The present study is confined to the upper part of this catchment. The study catchment called Munyu, is approximately 5 590Km ^{2}. It is bounded by the parallels of latitude 0 ° 50 ' S and 1 ° 50 ' S, and the meridians 36 ° 30 ' E and 37 ° 15 ' E. The Ngong Hills are to the west and the highest points are observed to lie between 2 360 – 2 460 meters Above Mean Sea Level.

The catchment can be divided into three main reaches namely, the upper, middle and lower reaches. The catchment supports an expansive population including the capital Nairobi and the densely populated districts of Kiambu and Machakos. The port of Mombasa and the coast north to Malindi lie outside the catchment, but rely on water supplies imported from it. In sustained drought conditions, Mzima springs and Sabaki river abstractions could meet the demand of Mombasa until the mid 1980's (Wain, 1983). This means that the present flow of the river system is already wholly committed, and that there is no reliable surplus to support new developments in the lower reaches. Further development requires the installation of dams and this must go together with sediment yield studies for a sustained reservoir capacity. One of the many factors given consideration in the development strategy for the Athi River relates to current and future rates of sediment transport as sediment depositions in reservoirs reduce live storage volume and yield. Reservoir developments must go hand in hand with catchment rehabilitation, soil conservation measures and sediment transport studies.

The subcatchment (3DA2) lies within the upper reach of the Athi-River Catchment, see Figure 1.0. The rivers in this study catchment mostly flow northeasterly but there are numerous tributaries that flow mostly in the southeasterly direction. The tributaries originate from the southern end of the Nyandarua Ranges. The Nyandarua Ranges are underlain by volcanic rocks that do not weather fast to yield soils that are highly erodible. But at present the extensive clearing of forests in Nyandarua to pave way for agricultural activities, population increase and constructions is not sustainable.

These land use changes have resulted into increased soil erosion and sediment yield. Unless soil erosion and sediment transport are arrested, the availability of the river water resources within the entire Athi River catchment will diminish greatly.

There were only eight gauging stations for water discharge and suspended sediment in the Athi River during the study period 1980 to 1981. Since then no continuous data is available on suspended sediment in this catchment. These stations are shown in Table 1.0 and can be seen in Figure 1.0.

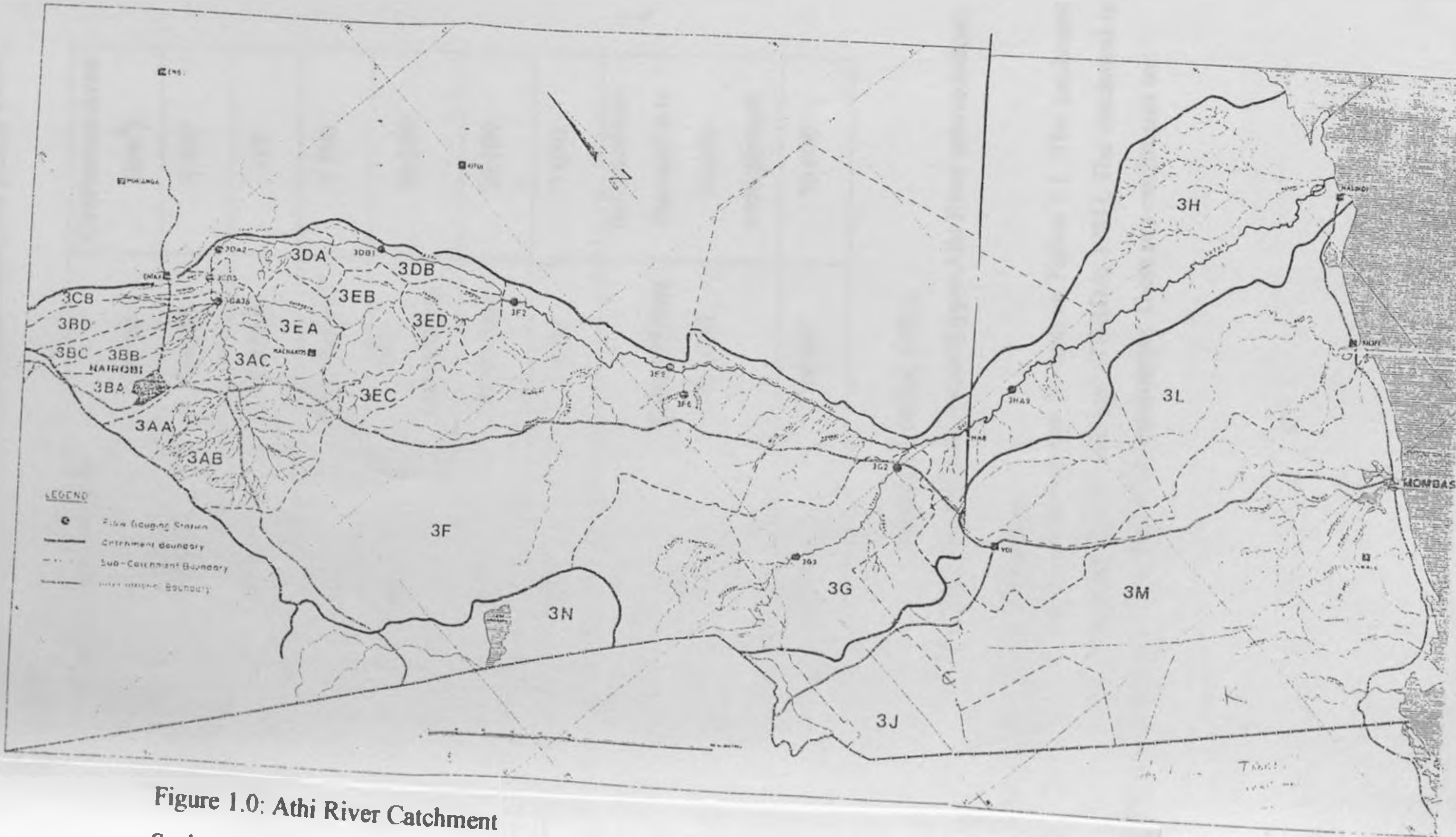

Figure 1.0: Athi River Catchment

Scale: 1: 1000 000

Source: TARDA, 1981.

Table 1.0: Gauging Stations in the Athi River Basin during the period 1980 to 1981.

Gauging Station Code Number	**River**	**Catchment Area (km^2)**
3BAB2	Nairobi	1 942
3CB5	Ndaragu	313
3DA2	Athi (Munyu)*	5 590
3F2	Athi (Mavindini)	10 200
3F5	Stony Athi	20 100
3G2	Tsavo	7 050
3GB	Tsavo (Mzima springs)	Indeterminate (because it is mostly underground)
3HA6	Sabaki	38 600

Source: (TARDA, 1981)

* This is the study subcatchment (Upper Athi River subcatchment)

1.2.1 The Athi River Catchment

A map of the Athi River Catchment can be seen in Figure 1.1. The catchment covers an area of approximately 67 000 km^2 (TARDA, 1981). The catchment is further sub-divided into five major sub-catchments. These sub-catchments are: -

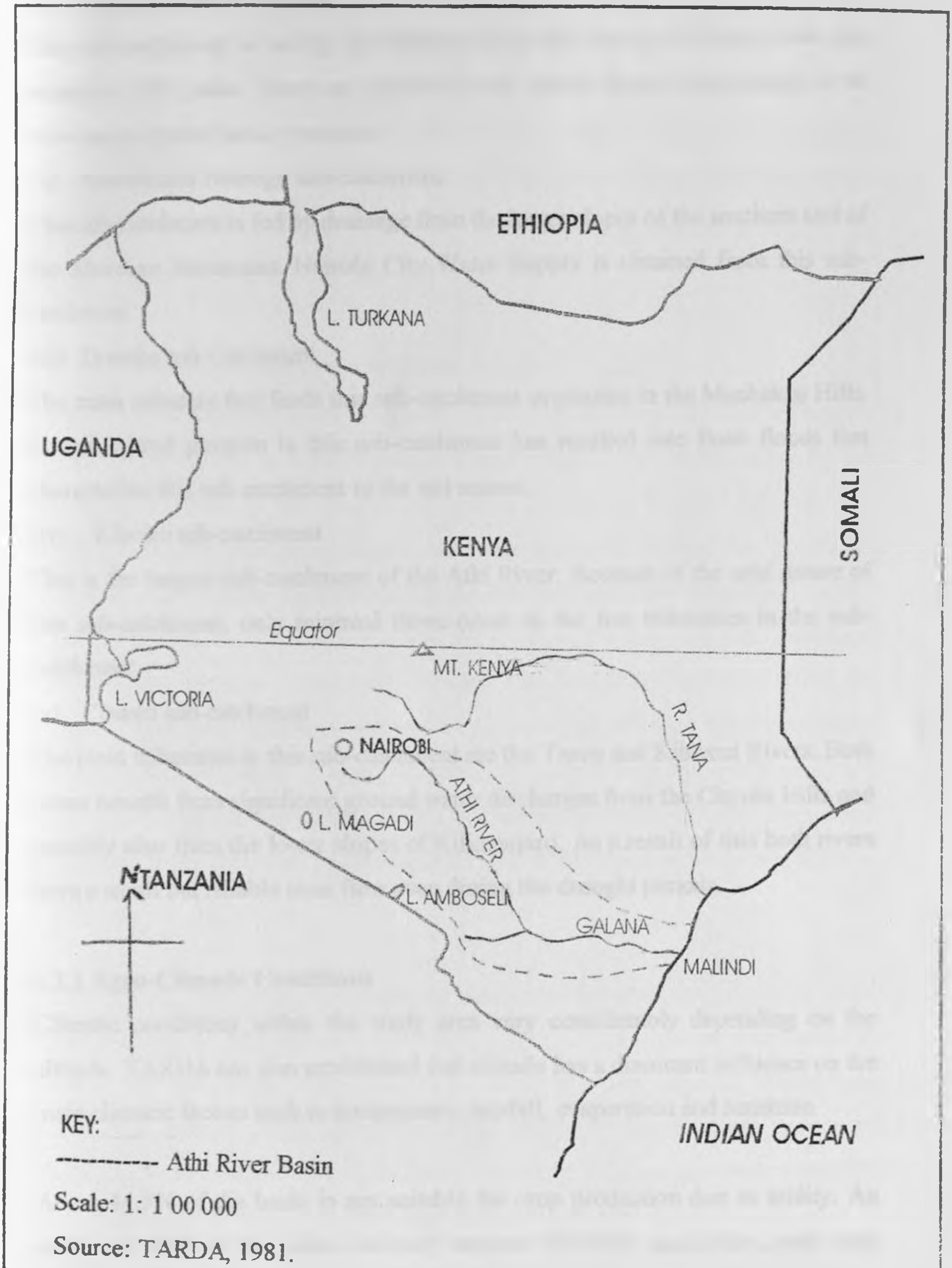

FIGURE 1.1: Map of Kenya Showing the Study Area

(i) Stony Athi sub-catchment

This sub-catchment is fed by the drainage from the Ngong Hills and from the extensive Athi plains. There are significant wet season flows, but minimal or no flow occurs during the dry seasons.

(ii) Nairobi and Ndaragu sub-catchment

This sub-catchment is fed by drainage from the lower slopes of the southern end of the Aberdare Mountains. Nairobi City Water Supply is obtained from this sub-catchment

(iii) Thwake sub-Catchment

The main tributary that feeds this sub-catchment originates in the Machakos Hills. Intensive land pressure in this sub-catchment has resulted into flush floods that characterize this sub-catchment in the wet season.

(iv) Kiboko sub-catchment

This is the largest sub-catchment of the Athi River. Because of the arid nature of this sub-catchment, only minimal flows occur in the few tributaries in the sub-catchment

(v) Tsavo sub-catchment

The main tributaries in this sub-catchment are the Tsavo and Kibwezi Rivers. Both rivers benefit from significant ground water discharges from the Chyulu Hills and possibly also from the lower slopes of Kilimanjaro. As a result of this both rivers have a small but reliable river flow even during the drought periods.

1.2.2 Agro-Climatic Conditions

Climatic conditions within the study area vary considerably depending on the altitude. TARDA has also established that altitude has a dominant influence on the main climatic factors such as temperature, rainfall, evaporation and sunshine.

About 44.5% of the basin is not suitable for crop production due to aridity. An additional 40% of the basin can only support minimum agriculture, with crop failure expectancy of 1 in 2 years. Only 15.5% of the basin has agro-climatic conditions suitable for crop production (TARDA, 1981).

Almost all agriculture practiced in Athi Basin is rain-fed. There is very little irrigation practiced in the basin. The main crops grown are maize, sorghum, beans, cowpeas, cassava, vegetables, fruit trees, coconut, cotton, sugarcane, coffee, tea, pyrethrum, sisal and cashew nuts (TARDA, 1981).

1.2.3 Sediment Studies in the Athi Basin before 1980

Edward calculated suspended sediment yields for 41 river stations in Kenya, (Edward, 1979). These stations included some from Athi River, which is the catchment under study. The calculated yield for the Athi at fourteen falls was 42 t $/km^2/yr$, while the other stations gave values in excess of 500 $t/km^2/yr$. The figure at Fourteen Falls could be attributed to the fact that the sub-catchment is mostly made up of volcanic rocks that are difficult to erode. Further, this sub catchment has not undergone so many land changes. The suspended sediment yield for Kalundu River near Machakos (Figure 1.2) is given as 546 $t/km^2/yr$. The Maruba sub-catchment that is in Thwake (Figure 1.2) gave a sediment yield of 1 500 $t/km^2/yr$. These figures are preliminary estimates values only as the catchment has undergone many activities. In all cases estimates were based on the period 1958 to 1974.

Results from the small representative and experimental catchment at Iiuni (Machakos) in the Thwake sub-catchment (Figure 1.2) gave annual total sediment yield of 535 $t/km^2/yr$ (Thomas et al, 1981). However, monitoring took place in one wet season only, in which rainfall was approximately one third of the annual mean. The total load recorded in the measurement period was up-scaled by a factor of three in order to provide a preliminary mean annual estimate.

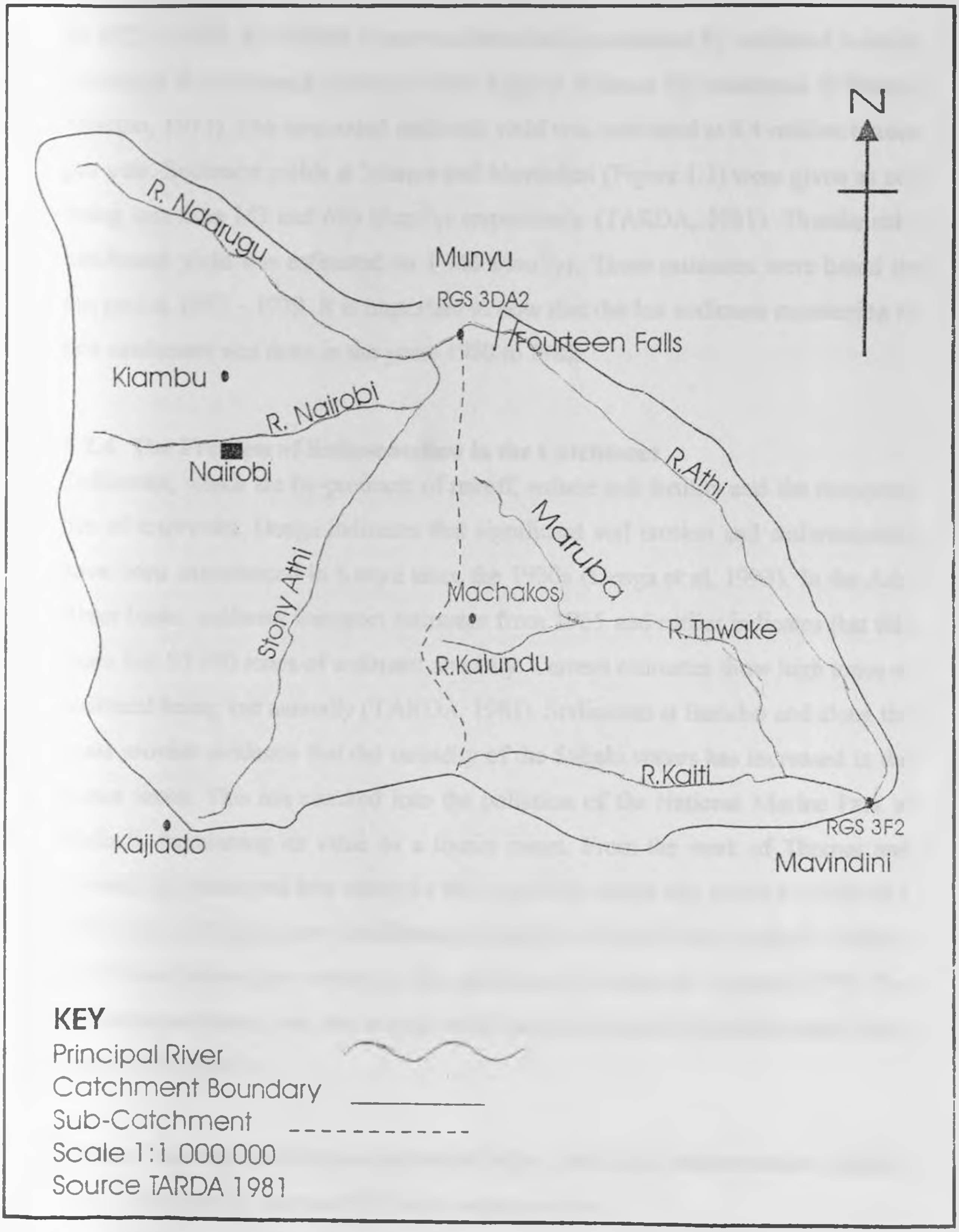

Figure 1.2: Map Showing the Study Area

In 1972 – 1973, the Sabaki River was intensively monitored for sediment in order to design the proposed Baricho Water Supply Scheme for Mombasa (Mansell-Muollin, 1973). The suspended sediment yield was estimated at 8.4 million tonnes per year. Sediment yields at Munyu and Mavindini (Figure 1.2) were given as not being less than 143 and 696 t/km^2/yr respectively (TARDA, 1981). Thwake sub-catchment yield was estimated as 1 366 t/km^2/yr. These estimates were based on the period 1957 – 1979. It is important to note that the last sediment monitoring in this catchment was done in the years 1980 to 1982.

1.2.4 The Problem of Sedimentation in the Catchment

Sediments, which are by-products of runoff, reduce soil fertility and the economic life of reservoirs. Denga indicates that significant soil erosion and sedimentation have been experienced in Kenya since the 1930s (Denga et al, 1993). In the Athi River basin, sediment transport estimates from 1965 and earlier indicates that this basin lost 55 000 tones of sediment annually. Current estimates show high tones of sediment being lost annually (TARDA, 1981). Sediments at Baricho and along the coast provide evidence that the turbidity of the Sabaki waters has increased in the recent times. This has resulted into the pollution of the National Marine Park at Malindi, threatening its value as a tourist resort. From the work of Thomas and Edward, the mean soil loss value for the Athi River Basin was found to be about 1 400 t/km^2/yr; this is above the allowable loss of 1 000 t/km^2/year given by Thomas and Edward when they worked on the catchment (Thomas and Edward, 1979). The maximum sediment loss rate occurs in the sub-catchment of Machakos and it was about 6 600 t/km^2/yr.

Some of the major problems experienced in the river due to sedimentation include:

- Reduction in reservoir life due to sedimentation.
- Turbine operation is adversely affected.
- Water pumps are adversely affected.

- Intake structures and irrigation canals have silted up.
- River channel sediment deposition clogs the river. This means that water becomes difficult to obtain especially during the dry season. This will result into fish population being drastically reduced.
- The deposition of fine sediments at the river mouth results in mud floods. These mud floods will be colonised by mangrove vegetation. Malindi beach has been extended in the last 20 years as a result of this deposition (Wain, 1983). For much of the year, the water of the beach is too loaded with fine silt, making it less attractive for beach tourism.

1.2.5 Sediment Problems in other Catchments in the Country

Although the problem of soil erosion and sedimentation in Kenya was identified in 1935, sediment yields monitoring only started in 1948 to 1965 (Denga et al, 1993). Between 1948 and 1965, the Colonial Government had established a network for monitoring sediment yields in catchments country wide. Between 1949 and 1966, a total of 7 933 samples were collected from a total of 275 gauging stations (Bobotti, 1978).

The problems faced during this time included:

1. Lack of standard procedures for sampling the sediment.
2. Lack of the measurement of the corresponding discharges at the time of the sampling. During the period 1947-1966, out of the 7 933 samples collected only 907 samples had the corresponding discharge measurements made at the time of the sampling (TARDA, 1981).

Another major contribution to sediment yield studies in East Africa was from East Africa Agricultural and Forestry Organization (EAAFRO), which established four experimental catchments at Kericho and Kimakia (Kenya), Atumatak (Uganda) and Mbeya in Tanzania (TARDA, 1981). These were set up in 1957 and were monitored for sediment yield among other hydrological variables. Both Mbeya and Atumatak stations stopped functioning in 1969 and 1970 respectively. But Kericho and Kimakia still continue to operate. Iiuni in Machakos was added to these gauging stations in 1976 as a "Representative Catchment Project (RCP)" with the assistance of the UK Ministry of Overseas Development, but when this assistance was discontinued the Iiuni station ceased to operate between 1980 and 1981 (TARDA, 1981).

Dunne has also compiled some useful information on the suspended sediment load on 97 river gauging stations in Kenya using regression analysis based on the 1948-65 sediment load and flow data (Dunne, 1975). Only suspended sediment load was monitored. No attempts were made to monitor the bed load. This suspended sediment load was regarded to reflect the total sediment load of the rivers, which is not true. Other works were those of Ongwenyi, who investigated 13 stations for river gauging and sediment sampling (Ongwenyi, 1978). Nine of these were part of a country wide river gauging network operated by the Ministry of Water Development. He established four additional stations for the purpose of his PhD study. Ongwenyi measured the bed load and carried out an assessment of the bed load using the Einstein bed load function. This function predicted the bed load of the order of 6% of the total sediment load in the Tana catchment

Sediment yields from some of the catchment for the period 1948 to 1965 are shown in Table 1.1. The highest rates of sediment yield are encountered in areas of very steep slopes such as the eastern sides of Mount Kenya, where cultivation is practiced on the steep valley slopes; and on the gentler but drier hill slopes in the lower marginal parts, where grazing occurs. In areas of undisturbed forests, sediment yields are extremely low.

Other studies carried out by, Dunne, Ongwenyi, Dunne and Ongwenyi indicate that there has been an increased rate of sedimentation in the multi-purpose reservoirs constructed along Tana River (Dunne and Ongwenyi, 1976; Dunne, 1978; Ongwenyi, 1978). They gave a figure of 2.6×10^6 m^3 of sediment to have been deposited in the Kindaruma reservoir since 1968. Wain and Edward also carried out some work in various catchments in the country and showed high rates of sediment yield and siltation of reservoirs and streams (Wain, 1983 and Edwards, 1979)

Table 1.1: Sediment yields from selected catchment areas in Kenya

Catchment	Area, Km^2	Area rate of Sediment loss, $t/km^2/yr$	Land-Use Type
Sagana, Above Kiganjo	501	8	Forest-use type
Sirimon, Above the Isiolo Nanyuki Road	62	9	Forest, steep slopes
Sagana, Above Sagana Town	2 650	35	Forest, steep slope and Agriculture
Nzoia, Above Webuye Falls	8 500	50	Forest/Agriculture
Tana, Above Kamburu Dam 4DE3	9 500	637	Forest/Agriculture
Chania, Above Thika	517	159	Agriculture/ Forestry
Thiba, Above Machanga	1 970	158	Agriculture/ Forestry
Tributaries of Athi, Nairobi, Machakos Area	510	216	Agriculture/ Forestry
Kambure, Above Main Nzoia River	1 350	105	Agriculture/ Forestry

Tana, Between grand falls and Garissa	15 200	1 579	Grazing
Tana, Between Sagana and Kindaruma	7 700	3 117	Agriculture/ Grazing
Ewaso Ng'iro, Above Archer's Post	15 300	1 569	Grazing

Source: (Denga et al, 1993)

The figures in the above table are based on the period prior to 1965 and may have increased due to changes in land use.

Ching also did some work in the Nyando catchment using insufficient data collected in the early 1940s and 1950s (Ching et al, 1999). He estimated the sediment load for Sondu Miriu and Nyando rivers as 150 and 425 t/km^2/yr, respectively. However, these estimates do not reflect the considerable changes in land use that have taken place in the catchment. He gave the examples of Kano Plains and Bundalangi flood problems to be as a result of erosion and sedimentation of river channels and other water carrying bodies.

1.2.6 Latest Issues on Sediment Studies in the Country

Because of lack of funds there have not been any regular programme to gauge or sample sediments in the rivers in Kenya beginning from the year 1986. A proposal was submitted in 1978 to establish 184 sediment-gauging stations at runoff gauging stations, but this is yet to be implemented

The most recent studies on river sediment transport in the country are those carried out in the mid-1980s. Sutherland and Bryan carried out investigations in a 31 ha ephemeral river catchment in the Baringo District in the Rift valley (Sutherland and Bryan, 1986). They gauged the runoff using a data logger and a float activated wastewater sampler that collected suspended sediment samples automatically. Between 1983 and 1985 HR Wallingford UK, TARDA, Ministry of Water Development and Kenya Power and Lighting Company Limited also carried out a study on sediment discharge movements at Sagana on the Sagana River (Charania, 1988). The river is the most important tributary to the Tana River and has a catchment area of 2 365 Km^2. The purpose of this study was to provide data that was necessary to estimate the siltation in the hydropower reservoirs on the Tana River. Other similar works are those done by Charania. He studied the frequency of the sediment sampling in the upper Tana River basin. A flow duration curve analysis method of assessing the annual sediment yield showed that more than 95% of the annual sediment yields are contributed by the runoff in the months of October, November, May and June. The Department of Agricultural Engineering at the University of Nairobi has also carried out research on the Athi River sedimentation. The University research is still on going.

Nordin has made the following general remarks on sediment problems (Nordin, 1991):-

1) Sediment problems associated with the construction of dams and reservoirs on sediment-laden streams cannot be eliminated. They have to be managed.
2) The theoretical and empirical basis to develop strategies for managing sediment problems exists. For example in the use of mathematical models to assess reservoir sedimentation.
3) Sediment management should involve planners, dam designers, managers and economists, who ultimately make the major decisions on projects.

1.3 OBJECTIVES

1.3.1 Main Objective

The main objective of this study is to estimate the total suspended sediment load from the Upper Athi - River sub-catchment, which is within the Athi River Catchment.

1.3.2 Specific Objectives

The specific objectives of the study are: -

Objective No. 1

To determine the sediment rating equation for the river at sediment measuring station number 3DA2 in the study area. This equation will be used to estimate the total sediment load that passed the gauging station during the study period.

Objective No. 2

To develop the parameters of the Instantaneous Unit Sediment Graph (IUSG) Model for the sub-catchment.

Objective No. 3

To estimate the annual suspended sediment load from the subcatchment using the IUSG model developed.

1.4 JUSTIFICATION

Edward calculated suspended sediment yield for various rivers in the country, including Athi River (Edward, 1979). He used the method of sediment ratings and flow duration curves, which has weaknesses compared to the model to be used in this study (IUSG). First, the method underestimates sediment loads in floods. Secondly, the method is inexact and only gave preliminary estimates of suspended sediment yield. Third, he used the rating equation in the form of $C = \alpha q^{\beta}$. This means that he did not consider the variance of the error term associated with rating equations when dealing with hydrological data, which has been found to be statistically significant in giving good estimates, as hydrological data are log-normally distributed (Annadale, 1987). Fourthly, Edward's method does not consider the catchment parameters which characterise the catchment's response to rainfall with reference to the rainfall duration and catchment geomorphology. It is these weaknesses, therefore, that prompted the hydrologists to apply the concept of Instantaneous Unit Hydrograph (IUH) as used in runoff estimation to sediment yield estimation using the Instantaneous Unit Sediment Graph (IUSG). The IUSG can be used in estimating sediment yield as it has been found to give good results, because it treats the catchment as a linear reservoir and considers the catchment's parameters. The IUSG conceptual model has also been found to give good estimates of sediment lost as compared to other methods (Rendon-Herrero, 1975). The IUSG model only forecasts suspended sediment yield, and not bed load. It is expected that the IUSG model will perform well in this study because the bed load is negligible in Kenyan streams (Dunne, 1979).

The IUSG is also a parsimonious model that involves the deterministic of two model parameters only. It is hence easier to fit this model using limited data available on sedimentation in Kenyan catchments. This justifies why it is the model used in this study.

CHAPTER TWO: LITERATURE REVIEW

2.0 Determination of Catchment Sediment Yield

This Chapter will discuss some of the common models currently used to estimate sediment transport. The chapter will discuss their limitations and will give the basis upon which the study model was selected.

2.1 Introduction

Gauging and modeling are the two basic approaches for determination of sediment yield of a catchment. In the gauging approach, the measurements of water discharge and sediment concentration of the stream serving the catchment are made through some suitable measuring devices. Accuracy and precision of the determined yields can be improved by increasing the frequency of the measurements, though this has a direct bearing on the costs. There are several procedures of gauging the sediment concentrations using bottle samplers. The commonly known procedures are Equal Transit Rate (ETR), Equal Discharge Interval (EDI), Grab Sampling (GS) and Automatic Single Stage Sampling (ASSS). The water discharges are measured concurrently with sediment concentrations. The measured discharges and concentrations are subjected to some computational procedures such as temporal concentration graph method or flow duration sediment rating curve method in order to derive the sediment yields

The modeling approach is cheaper and faster to determine the catchment sediment yields, but this requires calibration of the model that is being used (Sharma, 1994). The calibration exercise also needs field data, which must be collected through some representative procedure of sampling. A variety of models have been put forward for use, either for direct evaluation by involving the gross erosion and by calculating sediment delivery ratios. Sediment simulation can also be obtained from watershed hydrologic models. The models gaining currency are based on the

Linear Systems Theory (LST), Routing Concepts (RC), Digital Watershed Hydrologic Modeling (DWHM) and Stochastic Approaches (SA). Some other sediment models to date involve the use of Sediment Rating Curves (SRC), Empirical Equations (EE) and Modified Universal Soil Loss Equation (MUSLE).

Digital hydrologic models are largely deterministic and make use of mathematical equations of hydrological and erosional processes with some inclusion of empirical relationships. Some catchment models are also based on the sediment transport theories applicable in the river channels (Sharma, 1979). These theories are based on hydraulic principles and utilize the basic law of hydrodynamics. The physical models based on the concepts of hydraulic similitude can also be regarded to fall in this category. The sediment load in a river or stream is regarded to be composed of suspended and bed load components. The bed load component is better related to hydraulics of flow and can be modeled by the laws of hydrodynamics. The suspended component is poorly linked with the hydraulic parameters, as it is highly supply constrained. In short, hydrologic and hydraulic based models are being tried with some degree of success in modeling catchment sediment discharges. Stochastic models make use of the probability laws and are capable of providing values of sediment yields over a period of time. They can further relate the specified sediment yields with the return periods.

2.2 Determination of Sediment Yield by Gauging

Because the techniques for practical measurement of sediment are very laborious and expensive, samples must be drawn off the streams to be treated in the laboratories before sediment analysis is done. To reduce the expenses involved only periodic sampling of sediment transport at various points of a stream are taken. These sample results are then used to develop sediment transport forecasting and prediction models for the catchment. In this section, the two gauging methods used in the study to estimate sediment transport will be discussed. The methods are called the Sediment Time Concentration Graph and the Sediment Rating Curve. The factors that underlie their preference over the other methods will be given.

2.2.1 Sediment Time Concentration Graph

In this method, the mean sediment concentration sampled at a cross-section as well as the water discharges are correlated with the mean sediment at that point. The resulting model is of the form,

$$Q_s = K_c{*}Q{*}C \text{ -- } 2.0$$

Where,

Q_s = Sediment discharge (t/day)

Q = Daily mean water discharge (m^3/s)

C = Daily mean concentration of suspended sediments (Mg/l)

K_c = 0.0864 (conversion factor)

Equation 2.0 predicts Sediment Transport loss on a daily basis. To obtain sediment loss over a longer period of time, Ranga indicated that Equation. 2.0 must be integrated (Ranga Raju. et al, 1985).That is,

$$\frac{dQ_s}{dt} = K_c \frac{dQ}{dt} C \text{ -- } 2.1$$

Assuming the sediment concentration C is a function of the discharge Q, and further that this function is of the simple form,

$$C = \beta Q, \quad \text{If } \beta = \text{constant} \text{ -------------------------------- } 2.2$$

Then Equation (2.1) becomes,

$$\int_0^{Q_s} dQ_s = \int_0^{Q} K_c \beta Q dQ \text{------------------------------------} 2.3$$

$$= \int_0^{Q} K_c \beta Q dQ$$

$$Q_s = \alpha Q^2 \text{ ------------------------------------ } 2.4$$

Once the constant α in Equation 2.4 has been determined, the more readily available flow discharge measurements can be used to estimate the sediment loss from the catchment. Equation 2.4 shows that sediment transport is doubly sensitive to discharge. Therefore, if discharge doubles then sediment loss would increase by four times.

It is this extreme sensitivity of this model that made the author rejects it in this study. This is because minor errors in flow estimation or fluctuations upstream can lead to high errors in sediment estimation downstream.

2.2.2 Sediment Rating Curve

In the second model, the sediment yield is estimated from a mathematical function of the following type,

$$Q_s = aQ^b \text{ -- } 2.5$$

Where: -

Q_s = Instantaneous sediment discharge (t/day)

Q = Instantaneous water discharge (m^3/s)

a and *b* are empirical constants

The parameters *a* and *b* in the sediment rating curve can be obtained from a log-log plot of sediment and water discharge data. This will plot out as a straight line (Vansickle and Beschta, 1983).

We then develop a long time water flow duration curve for the station. The sediment rating curve is then applied to the flow duration curve. The resulting computation gives a long term average yield. A correction factor is applied to the suspended sediment yield and the total sediment yield is then obtained.

From the sediment rating curve, we can develop the sediment rating equation. This will take the form shown below: -

$$C = \alpha q^{\beta} Z \text{ --2.6}$$

Where

C = Sediment concentration (mg/l)

q = Water discharge (m^3/s)

α and β = Empirical parameters

Z = Error term

The parameters α and β will be obtained using the method of Ordinary Least Squares (OLS) and by applying a logarithmic transformation of C and q.

When the value of Z is not included in this equation, then it allows for a straight forward prediction of C. But this has resulted in underestimation of catchment sediment yields as it does not consider the value of Z (error term). There has been a tendency to assume that the expected value of Z is 1, which is not the case (Sharma, 1993). A better estimate of Z is obtained by linearization of equation 2.6.

The linearized form of Equation. 2.6 is: -

$$\ln c = \ln \alpha + \beta \ln q + \ln Z \text{ ------------------------------------2.7}$$

Z is a random variable that can be described using a Normal Probability Distribution Function (PDF). Statistically the value of Z can be estimated as follows: -

$$Z = \exp\left(0.5Se^2\right) \text{------------------------------------} 2.8$$

Where,

Se = Standard error.

This is given by

$$Se^2 = \frac{1}{n(n-2)} \left(S_{xy} - \frac{S_{xy}^{\ 2}}{S_{xx}}\right) \text{--------------------------} 2.9$$

Where,

S_{xy} is the variance of x and y

S_{xx} is the variance of x

n is the sample space

This model is a better predicting tool for sediment transport than the one discussed in section 2.2, because it accounts for the statistical variation of the sediment with flood flow. The statistical dependence of the estimated parameters is a further advantage of the model because it can be used to estimate the reliability of the parameters. Lastly, the author also selected the model because of its parsimony, that is, few parameters that are easier to estimate.

2.3 Sediment Transport Prediction and Forecasting Using Models

While the present study is restricted to the suspended sediment, it is important to note that this sediment is related to the total soil erosion on the catchment. This relationship is captured by the Sediment Delivery Ratio (SDR) which will be discussed in this section. The SDR method is pertinent to discuss here because some of the studies done earlier and which the author used in assessing these works were done on catchment erosion.

2.3.1 Factors That Affect Selection of a Model

According to Sharma, there are various sediment yield models available for making predictions to solve specific problems namely (Sharma, 1994);

- Erosion control planning
- Water resources planning and design
- Water quality modeling

Some of these problems can be solved with simple models but others require complex models (Sharma and Dickinson, 1979). The choice of what model to use will depend on the following:

(i) The duration of the storm

In situations where life could be endangered by high concentrations of sediments, storm based modeling of sediment concentrations is required to ensure that these concentrations will not last more than a critical duration.

(ii) The catchment size

Hydrologically, large catchments exhibit less heterogeneity than small catchments. For example, an isolated extreme rainfall event in a small localized zone may only affect the flows in the local tributary but will have little overall effect, as the catchment will average out extremes in the various sub- catchments. This enables the catchment behavior to be modeled using few- parameter models.

(iii) Sediment sources

The number and types of sediment sources within a basin and their relative importance dictate the modeling requirements. Gullies contribute large amounts of sediment per unit area. Such sediment is readily available for transport because gullies are generally located at the head of channel systems. Likewise, sediment contributions from roadsides and ditches are often appreciable. Construction sites are also potential extreme sources of catchment erosion.

In the succeeding section, common sediment prediction and forecasting models will be discussed. The choice of which model to use will also be discussed.

2.3.2 Sediment Delivery Ratio Method

The soil particles detached, transported and deposited to other places is referred to as erosion. It is true that all eroded materials from the catchment do not get into the stream system as some remains on the catchment. The soil particles detached from comparatively level fields, with little or no surface runoff, move only for shorter distance and are not transported to downstream points in the catchment. On the contrary, the soils eroded from steep lands can be carried to the stream system and be transported for long distance. The amount of eroded material which completes the journey from the point of origin to the downstream control point, such as a reservoir, is known as the sediment yield (Suresh, 1997).

SDR is defined as the fraction of gross erosion that is transported from a given basin as sediment yield.

That is:

$$SDR = \frac{\text{Sediment yield}}{\text{Gross erosion}}$$

The value of SDR is always less than one, because sediment yield is less in magnitude than the gross erosion.

The Sediment Delivery Ratio (SDR) method of predicting sediment yield is widely used throughout the world. Garde and Kothyari have used it to predict sediment yield in the Yellow River in China, while Dunne has used it on various rivers in Kenya. Das also pointed out that it is a convenient and adequate method for those problems that require an estimate of the average annual sediment yield, especially sediment pools in reservoirs (Garde and Kothyari, 1987; Dunne, 1978; Das, 2000). Some measurements carried out by Dunne and Garde and Kothyari in India showed that as little as 5% and as much as 90% of the materials eroded in some catchments can be delivered to a downstream point.

Applying a delivery ratio to estimate gross erosion can be a fairly accurate technique of predicting downstream sediment yields if delivery ratios can be determined with accuracy. The efficiency of a stream system to transport the eroded materials from the origin source to a downstream point of measurement helps to determine SDR. Sediment delivery ratios are related to basin and climate characteristics. The factors that determine SDR are discussed in section 2.3.3 below.

2.3.3 Factors Affecting Sediment Delivery Ration (SDR)

a) Land Use

Garde and Kothyari's studies in India have indicated that land use is the most influential factor affecting sediment yield followed by catchment slope, rainfall intensity and drainage density. Similar findings are reported in Kenya, where, Dunne has shown that land use is the main factor affecting the sediment yield. However, such findings are difficult to quantify, and SDR is still largely derived from the catchment size as in Equation 2.10,

$$SDR = \alpha A^{-\beta} \qquad \text{------} 2.10$$

In this equation, SDR is related to the Catchment Area (A) through some power law relationship. SDR decreases as the catchment area increases.

b) Size of the Catchment

The size of the catchment area has a dominant effect on total sediment yield from catchment. However, it's relative importance with respect to influencing SDR and sediment production rate has been questioned. The rate of sediment delivery decreases as the size of the catchment increases. This is because the probability of entrapment and lodgment of the soil particles that are being transported downstream increases as the size of the drainage area increases. In addition, the probability of having a rainfall event that would cover the entire catchment is much greater for a small size catchment.

c) Topography

The important topographic features affecting the SDR are the degree and length of catchment slope. For a steep catchment, the SDR is higher.

d) Channel Density

The channel density, which is the number of channels per unit drainage area, has similar effect on SDR as the degree and length of catchment slope. That is, a catchment with well-defined channels has a high SDR.

e) Relief and Length of Catchment Slope

Studies have shown that, the effect of catchment slope is significant on sediment delivery ratio and sediment yield. Zachar found out that the rate of sediment delivery from 25 catchments in the Red Hills area of Texas was highly correlated with the relief ratio (Zachar, 1982). That is,

$$R = h/L \qquad (2.11)$$

Where,

L is the maximum length of the catchment (m) and h is the relief of the catchment.

He gave an equation given below,

$$SDR_e = 2.94259 - 0.82363 \log R \qquad (2.12)$$

Where

SDR_e = Estimated delivery ratio (%)

R = Relief ratio.

The relief ratio normally increases with decreasing area of sub – catchment in a given catchment

f) Precipitation

Precipitation affects both sediment yield and SDR. The rate of gross erosion is high when a high intensity storm occurs on the catchment at the time when cover conditions offer minimum protection against erosion. Lower erosion prevails when high intensity rainfall occurs during the period when ground surface is frozen or is fully covered with vegetation.

g) Runoff

The runoff rate affects the SDR and sediment yield significantly. The different factors to affect the runoff rate are the nature of precipitation, infiltration, antecedent moisture condition and physical characteristics of the catchment including topography and shape. If all the conditions were the same then the runoff rate would be greater from the steep sloped catchments. The greater the runoff rate or volume the higher the amount of sediment yield and vice versa.

While the SDR would be a powerful tool in estimating sediment transport, no studies have been carried on it in this country. Because of this lack of information on the SDR, the model developed in this study cannot be used to estimate catchment erosion.

2.3.4 Empirical Sediment Transport Prediction Equations

The majority of the works cited in this study refer to empirical modeling of sediment transport done in Kenya and other countries. Yet it is important to understand that there is a big difference between such empirical modeling and the deterministic modeling employed in these studies, which are discussed below.

Empirical equations have been proposed for the determination of sediment load carried by water in both open and closed channel flows. Since bed load is better correlated to flow dynamics, most of these equations tackle the determination of this component. These equations include those based on diffusion theory and gravitational theory as documented in Kinori and Mevorach and the energy balance theory as documented in Singh and Krostanovic. The problem with these equations is that they are area-specific and give accurate results only when used in the geographical locations in which they were developed (Kinori and Mevorach, 1984) and (Singh and Krostanovic, 1984).

Most of these equations were developed on the basis of the observed sediment yield and basin characteristics, such as meteorological factors (mostly rainfall and temperature), topographical data (e.g. average slope) and soil properties like soil texture, soil structure and soil pH. Land use and vegetation are often considered modifying factors. The equations consider the natural processes in an integrated way, offer a simple solution, generally require easily obtainable data and yield reasonable results for the similar conditions for which they were developed.

Some of the equations developed are due to Flaxman, Dendy and Bolton, and Garde and Kothyari.

Flaxman gave the following equation,

$$\text{Log}(S+100) = 524.2 - 270.7\log(X_1+100) + 6.41\log(X_2+100) -$$

$$1.7\log(X_3+100) + 4.0\log(X_4+100) + \log(X_5+100) \quad \text{-------------------} 1.13$$

Where,

S = Average annual sediment yield (t/mi^2)

X_1 = Ration of average annual precipitation (in) to average Temperature (^{0} F)

X_2 = Average basin slope (%)

X_3 = Soil particles greater than 1.0mm (%)

X_4 = Soil aggregation index (%)

X_5 = 5% probability peak discharge ($ft^3/s/mi^2$)

The five parameters are expressions of vegetative growth (X_1), topography (X_2), soil parameters (X_3 and X_4), and climate (X_5). The Flaxman's equation was developed in the US and it explains about 91% of the variance in the average sediment yield from 27 catchments ranging in size from 12 to 54m^2 in 10 western states, (Flaxman, 1972).

Dendy and Bolton also derived sediment yield equation from reservoir deposition data obtained from catchments throughout the USA. The derived equation was:

$$S = 1958e^{-0.055Q}\left(1.43 - 0.26\log_{10} A\right) \text{------------------------} 2.14$$

Which applies when runoff $0 < Q < 50$ in / yr.

Where,

S = Sediment yield (t / in /yr)

Q = Runoff (in)

A = Drainage area (mi ^{2})

(Dendy and Bolton, 1976).

Garde and Kothyari also gave the following relationship for Indian's catchments as:

$$S = 0.02P^{0.6}Fe^{1.7}S_L{}^{0.25}Dd^{0.1}(Z)^{0.19} \qquad \text{------------------} 2.15$$

Where: -

S = Average annual sediment yield (0.01 to 0.02 tonnes)

P = Average annual rainfall (63.77 to 381.11 cm)

P_{max}=Average maximum monthly rainfall (9.0 to 108.3 cm)

Fe= Erosion factor (0.28 to 1)

$$Z = \frac{P_{max}}{P}$$

S_L= Land slope (0.001 to 0.200)

A= Catchment area (43 to 82 880 km^2)

Dd = Drainage density (0.002 km^{-1} to 0.31 km^{-1})

The erosion factor Fe was defined as:

$$Fe=\frac{\left(a_1F_A+a_2F_G+a_3F_f+a_4F_w\right)}{A} \quad \text{------------------------2.16}$$

Where

a_i =Weightage factors i=1 to 4

A= Catchment area

F_A = Arable land

F_G= Grass and scrub land

F_w=Waste land

F_f= Forest land.

The catchment slope S_L was defined as: -

$$S_L=\frac{1}{A}\sum A_iS_i \quad \text{--2.17}$$

Where

S_i =Slope of the portion of the catchment having area A_i.

(Garde and Kothyari, 1987).

The margin of error on such empirical models is high because of their dependence on many variables which have their own individual errors. Furthermore such empirical models are difficult to apply because they require an accurate estimation of many parameters, especially from large catchments. It is an effort to tackle these limitations that led to the author to attempt a deterministic approach in sediment transport estimation.

2.3.5 Modified Universal Soil Loss Equation

The other researchers who have worked on the study catchment have largely used the Universal Soil Loss Equation (USLE) (Dunne et al, 1976 and Ongwenyi, 1978). Therefore, it is important to examine the theory of the USLE in order to understand the differences between the results obtained by these authors and those obtained in this study.

The MUSLE explained below is a stochastic-deterministic model that is relevant to the present study, much is on deterministic modeling. However, again little study has been done to enable a comparison with this study.

The Universal Soil Loss Equation (USLE) was developed in 1965, it can predict average annual sediment yield by applying a delivery ratio in large catchments, but the accurate estimation of delivery ratios is generally difficult at many places due to non-availability of measured data. The USLE is also not considered an appropriate model for water quality modeling. Such modeling requires shorter time increments than one year, as well as the consideration of both runoff and sediment parameters of pollutants (Wischmeier and Smith, 1978).

Williams modified the USLE equation by replacing the rainfall factor 'R' by a runoff factor $(Q.q_p)^{0.56}$ .This is done so that both soil erosion and sediment movement over the catchment are considered. He called the model the Modified Universal Soil Loss Equation (MUSLE). MUSLE makes it possible to calculate sediment on a storm-by-storm basis (Williams, 1975). Computer software is available to process both the USLE and the MUSLE. The equations are as below,

$$S_T=RKCPLS_L \quad \text{---} 2.18$$

$$S_T=95(Qq_p)^{0.56}\,KCPLS_L \text{-----------------------------------} 2.19$$

Where,

S_T= Storm sediment yield (tonnes).

Q= Storm runoff (mm).

q_p= Peak discharge (m^3/s).

K= Soil erodibility factor.

C=Crop management factor.

P= Conservation practice factor.

L= Length factor.

S_L= Slope factor.

Equation 2.19 can be applied to large catchments if sediment sources are uniformly distributed over the catchment and the channel tributaries are hydraulically identical. However, Suresh and Das pointed out that these conditions are not easy to find in most of these large catchments. Therefore, the equation is mainly applicable to individual storms on agricultural catchments of up to 70 Km^2 in area (Suresh, 1997 and Das, 2000).

Estimation of sediment yields by MUSLE equation from very large agricultural catchments is not very accurate due to variations in climatic factors, soil characteristics, land slope, crop management, erosion control practices and catchment hydraulics within the catchment area. Sediment yield from large catchments can be estimated more accurately if such catchments are divided into sub-catchments of less than 25 Km^2 in order to compensate for the non-uniformity within distributed sediment sources, and route the sediment yields from the sub-catchments to the outlets of the entire catchments. This will include effects of catchment hydraulics and sediment particle size (Das and Chauhan, 1990).

Williams proposed the following routing model for estimation of the sediment yield from large catchments. He made the assumptions that the sediment deposition is dependant on the settling velocity of existing sediments, travel time, particle size and amount of sediment suspension (Williams, 1975).

Williams expressed these assumptions mathematically as,

$$\frac{dy}{dt} = -BY\sqrt{D} \qquad \text{2.20}$$

Where,

y = Sediment yield at an individual channel section

t = Time

B = decay constant also called as routing co-efficient.

D = Diameter of sediment particles.

2.3.6 Instantaneous Unit Sediment Graph (IUSG)

The Instantaneous Unit Sediment Graph (IUSG) method formed the core of the study.

The Unit Sediment Graph is the graph that results from a unit of mobilized sediment occurring over specified time duration. The sediment graph is analogous to the Unit Hydrograph as used in operational hydrology (Williams, 1978). The unit of mobilized sediment has been generally taken as one metric tonne (1 000 kg). The relationship between hydrographs and sediment graphs was recognized as early as in the 1940's but was developed further in the 1970's (Rendon-Herrero, 1974). Application of the concept of the Unit Hydrograph to develop Unit Sediment Graph has been found to provide good results in sediment yield estimation by various investigators (Singh and Chen, 1982), and (Gikonyo, 1994). The Unit Sediment Graph is a pulse response function of a linear fluvial system. This can be modeled using the linear reservoir theory and by treating it as a lumped unsteady flow system. Various methods of deriving the USG are available.

The series graph is one such method that has been used successfully (Rendon-Herrero, 1975). Depending on the catchment characteristics, the peak of the USG can be found to precede, coincide or lag behind the runoff hydrograph peak.

To obtain the USG, a synthetic Instantaneous Unit Sediment Graph was developed and applied to sediment transport forecasting. The derivation of this model is given in Appendix 1 and is well documented (Sharma, 1999). In addition, an explanation is provided on how the parameters of the model will be obtained in section 2.3.8.

2.3.7 Derivation of the Nash Model

The derivation of the Nash cascade, which is extensively employed in analyzing the data in this study, is provided in Chow, Sharma and Shaw (Chow et al, 1988; Sharma, 1999; Shaw, 1988) and can be seen in Appendix 1.

The runoff process can be regarded as an outflow from a cascade of linear reservoirs. A linear reservoir is one in which storage (S) is linearly related to outflow q,

$$S = Kq \quad \text{--} 2.21.$$

Where,

S =Storage (m^3)

K = Storage recession parameter (hr)

q = Outflow rate (m^3/s or mm/hr).

The units employed in equation 2.21 are consistent, except that the units are given at the frequency at which the data is observed. For example, the flow is observed daily but its values are recorded in M^3/s.

The derivation of IUH is based on the convolution integral and is well explained in Appendix 1. The solution to equation 2.21 after the convolution integral is given in the following Gamma Function,

$$U(t)=\frac{1}{k\Gamma n}\left(\frac{t}{k}\right)^{n-1}e^{\frac{-t}{k}} \qquad \text{------------------------------}2.22$$

Where

U (t) = ordinates of the IUSG (tones/hr).

n = number of routing reservoirs.

k = storage constant of the reservoirs (hr).

The Nash model is a conceptual model that was designed for a finite integer number of reservoirs. Both the units of t and k must be the same (hrs). Therefore, the resulting ordinates of IUH will be in cm/hr or mm/hr. If the IUH ordinates are multiplied by the area of the catchment we get Q in m^3/hr. Therefore, for a given catchment, if proper values of n and k are known, then IUSG and hence TUSG can be computed.

The Gamma Function in Equation 2.22 is given by

$$\Gamma n=\int_0^{\infty} e^{-x}x^{n-1}dx \qquad \text{--}2.23$$

The values of Γn are obtained from standard Gamma tables and it's usually tabulated for values of n ranging only from 1.0 to 2.0 as can be seen in the Gamma Function table in, Appendix 2. The relationship in equation 2.24 can be used to evaluate Γn for any n either less than 1 or more than 2 (Das, 2000).

$$\Gamma\,(n+1)=n\,\Gamma n \qquad \text{--}2.24$$

The parameters n and k in the IUSG in equation 2.22 exhibit good correlation with the basin parameters like length of the stream, slope, area and vegetal cover. These variables have changed in our subcatchment due to an increase in population that has led to much urbanization and agricultural intensification. These changes have reduced the capacity of the catchment to store water for longer periods hence reducing the catchment recession constant k.

Even though UH is a handy tool when you want to study any catchment. It has got some limitations and assumptions which are not always true. These are,

i. The assumption of proportionality is strictly not seen in practice. It is applicable particularly to certain regimes of stream flow such as bank full or flood conditions. At low and medium flows, the law of proportionality or linearity does not hold strictly.

ii. The assumption of time invariance implies that whatever the point of time of occurrence of the storm, the response would be the same. The same amount of rainfall excess will take longer in appearing as surface runoff in wet season when the vegetation is at its maximum development and the hydraulic behaviour of the catchment will be rougher.

iii. The assumption of superposition postulates that the contribution from two succeeding pulses of rainfall is independent of each other. This is strictly not true, as the dependence has been largely evident in most of the hydrological processes, particularly on short time basis, where dependence is very pronounced.

iv. The other weakness of the Unit Hydrograph theory is the assumption that the rainfall excess is produced uniformly within time T period and over the area of the catchment. The areal distribution of rainfall is rarely uniform within a storm. Likewise the intensity of rain is not uniform throughout the storm period, at least within the period of "T" unit time chosen for unit graph analysis.

Despite the above limitations, the Unit Hydrograph is a useful tool for flood hydrograph estimation and synthesis. It can be applied for periods ranging from hours to a week or even up to 10 days basis. The catchment area could also be extended up to 10 000 Km^2. The main problems in the derivation of a Unit Hydrograph are the assessment of the rainfall excess from measured rainfall excess and the separation of the resulting surface runoff from the total hydrograph.

2.3.8 Evaluation of the Parameters n and k

The values of n and k were computed using the method of moments as well documented in Chow and Ranga Raju et al (Chow et al, 1988 and Ranga Raju et al, 1985). The first and second moments of the IUH about the origin at a time t = 0 are given as is explained below,

In general the m^{th} moment of any area about the origin is defined as,

$$m_m = \frac{\int_A f(x).dx.x^m}{\int_A f(x).dx} \text{ -- } 2.25$$

From the above definition the m^{th} moment of IUH about the origin is given by

$$m_m = \frac{\int_0^\infty (u)t.dt.t^m}{\int_0^\infty (u)t.dt} \text{ -- } 2.26$$

Since the area of the IUH is always unity then

$$m_m = \int_0^\infty (u)t\,dt\,t^m \text{ -- } 2.27$$

Therefore replacing the value of (u) t from Equation 2.22 we get,

$$M_m = \frac{1}{k\Gamma n}\int_0^\infty e^{\frac{-t}{k}} \left(\frac{t}{k}\right)^{n-1}.t^m.dt \text{ ------------------------- } 2.28$$

This becomes

$$\frac{k^m}{\Gamma n} = \int_0^\infty e^{\frac{-t}{k}} \left(\frac{t}{k}\right)^{n-1} \left(\frac{t}{k}\right)^{m} d\left(\frac{t}{k}\right) \text{ ------------------2.29}$$

If we replace (x) with (t) from the definition of gamma function in equation 2.23 we get equation 2.30 as,

$$\Gamma n = \int_0^\infty e^{-x} . x^{n-1} . dx \text{ ----------------------------------2.30}$$

Which is equal in expression when we replace (x) with (t) to the expression below

$$\int_0^\infty e^{-t} . t^{n-1} . dt$$

Therefore, the expression below is equal to Γ (m+n).

$$\int_0^\infty e^{\frac{-t}{k}} . \left(\frac{t}{k}\right)^{n-1} \left(\frac{t}{k}\right)^{m} . d\left(\frac{t}{k}\right) = \Gamma(m+n) \text{ ----------------------------2.31}$$

The solution to this integral is,

$$m_m = \frac{k^m \Gamma(m+n)}{\Gamma n} \text{ --2.32}$$

Since we are only evaluating two parameters (n and k), we need to calculate the first two moments only. From the equation above, m = 1, gives the first moment of IUH or IUSG as,

$$m_1 = \frac{k^1\Gamma(1+n)}{\Gamma n} \text{------------------------------} 2.33$$

And if $\Gamma(1+n) = n\Gamma n$ --2.34

Therefore, m_1 is equal to

$$M_1 = \frac{kn\Gamma n}{\Gamma n} = nk \text{------------------------------} 2.35$$

And for m = 2, we have

$$= k^2(1+n).\frac{n\Gamma n}{\Gamma n} \text{------------------------------} 2.36$$

$$m_m = \frac{k^2\Gamma(2+n)}{\Gamma n}$$

$$m_2 = n(1+n)k^2 \text{------------------------------} 2.37$$

The effect of routing the input through a series of linear reservoirs is to transform each elementary block of rainfall $I(\tau).d\tau$ into an elementary outflow as shown in Equation 2.38,

$$\frac{I(\tau)d\tau}{k\Gamma n} e^{\frac{-t}{k}} \left(\frac{t}{k}\right)^{n-1} \text{------------------------------} 2.38$$

This can be illustrated diagrammatically as in Figure 2.1.

The center of area of each elementary block is moved to the right by an amount nk, and the center of the area of the total outflow is also moved to the right by nk.

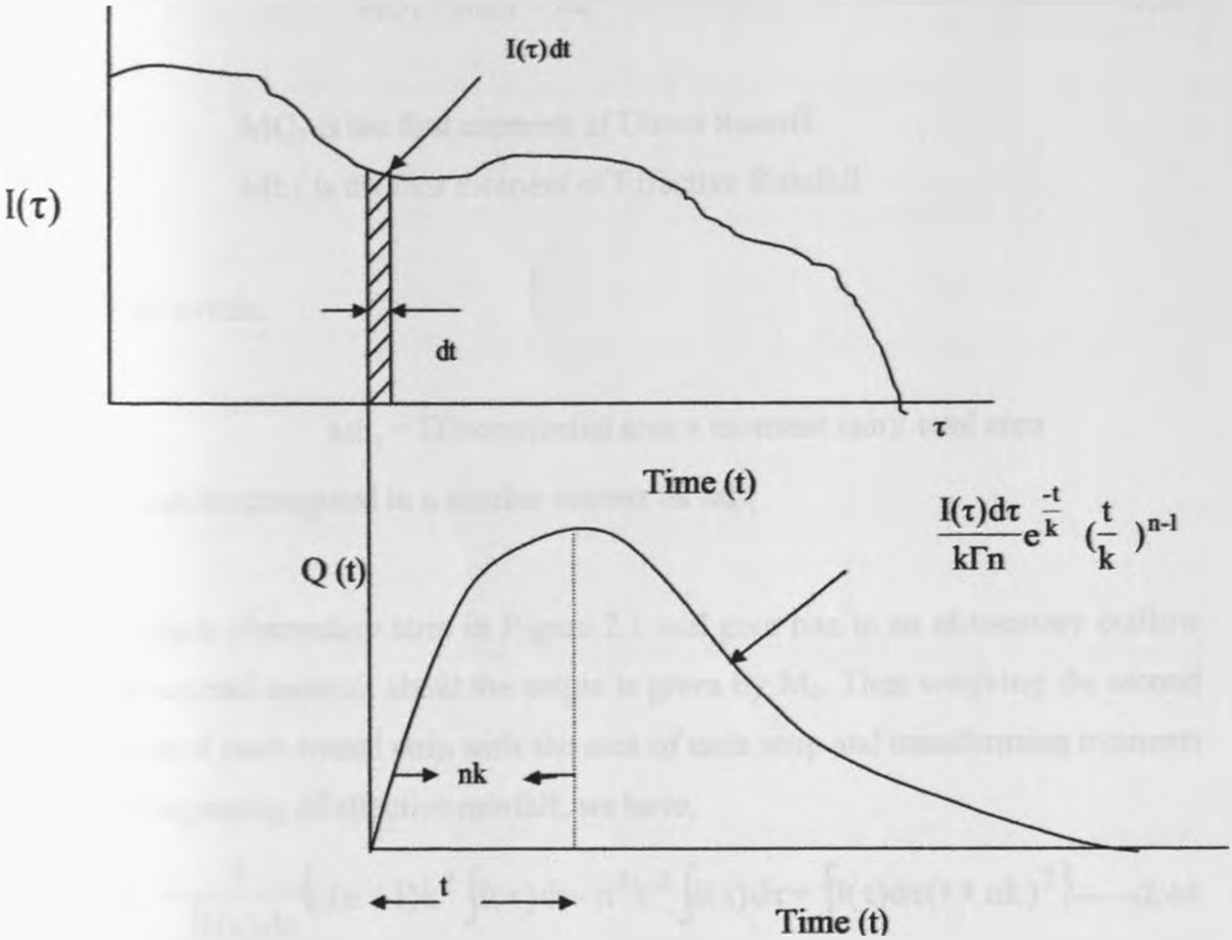

Figure 2.1: Rainfall Transformation into Runoff, (Linsley et al, 1988).

The first moment, M_1, represents the lag time of the centroid of the area under the IUSG. Applying the IUSG in the convolution integral to relate the Excess Rainfall Hyetograph (ERH) to the Direct Runoff Hydrograph (DRH), the principle of linearity requires that each infinitesimal element of the ERH to yield its corresponding DRH with the same lag time. In other words the time difference between the centroids of the area under the ERH and the DRH should be equal to

M_1 If M_1 is the first moment of the ERH about the time origin divided by the total effective rainfall and MQ_1 is the first moment of the DRH about the time origin divided by the total direct run-off.

Then,

$$MQ_1 - ML_1 = nk \qquad \text{---2.39}$$

Where

MQ_1 is the first moment of Direct Runoff

ML_1 is the first moment of Effective Rainfall

In other words,

$$ML_1 = \Sigma(\text{Incremental area x moment arm})/ \text{ total area}$$

MQ_1 can be computed in a similar manner as ML_1

Again each elementary strip in Figure 2.1 will give rise to an elementary outflow whose second moment about the origin is given by M_2. Then weighing the second moment of each routed strip with the area of each strip and transforming moments to the beginning of effective rainfall, we have,

$$MQ_2 = \frac{1}{\int I(\tau)d\tau}\left\{n(n+1)k^2 \int I(\tau)d\tau - n^2k^2 \int I(\tau)d\tau + \int I(\tau)d\tau(t+nk)^2\right\} \text{------2.40}$$

$$= n(n+1)k^2 - n^2k^2 + \frac{1}{\int I(\tau)d\tau}\int\left\{t^2 + n^2k^2 + 2tnk\right\}I(\tau)d\tau$$

$$= n(n+1)k^2 - n^2k^2 + \frac{\int I(\tau)d\tau t^2}{\int I(\tau)d\tau} + 2nk\frac{\int I(\tau)d\tau t}{\int I(\tau)d\tau} + n^2k^2$$

$$= n(n+1)k^2 + ML_2 + 2nkML_1$$

Rearranging the above expression we get Equation 2.41,

$$MQ_2 - ML_2 = n(n+1)K^2 + 2nkML_1 \qquad \text{------------------------------------2.41}$$

Where,

ML_2 Is the second moment of the Effective Rainfall about the time origin and MQ_2 is the second moment of Direct Runoff about the time origin.

The second moment of area can be calculated using the parallel axis theorem. That is,

ML_2= {$\sum$ (Incremental area *(moment arms)^2) + $\sum$ (Second moment about centroid of each increment)}/total area.

MQ_2 can also be computed in a similar manner as ML_2

Equation 2.39 and 2.41 are used to evaluate the value of n and k from observed rainfall and sediment runoff.

The suspended outflow hydrograph will be obtained by convolving U (t) with mobilized sediment $S_m(t)$ both in continuous and discrete form as used by Sharma (Sharma, 1999);

$$Q(t) = U(t) * S_m(t) = \int_0^t U(t-\tau) S_m(\tau) d\tau \qquad \text{-------2.42}$$

and,

$$Q_j = U_j * S_{mj} = \sum_{i=0}^{j} S_{mj-i} * U_i \qquad \text{------------------------------2.43}$$

Where,

$Q(t)$ = Sediment outflow hydrograph (t/hr)

$$S_m(\tau) = A_c E(\tau)$$

And,

A_c= Watershed area contributing to sediment outflow (km^2)

E = Mobilized sediment (t/km^2)

τ = Dummy variable of integration and is replaced by counter i in the discrete form.

2.3.9 Relationship between Mobilized Sediment and Rainfall Excess

For deriving the hyetographs, the rainfall data was obtained from the meteorological department. A sediment histogram was developed through regression analysis between excess rainfall (P_{net}) and mobilized sediment (S_m) of the form $S_m = aP_{net}^b$, where a and b are empirical constants. The excess rainfall (Pe) was changed into excess runoff using equation 2.44, which was developed by Vansickle (Vansickle et al 1983).

$$q = 0.278 PeA\, m^3/s \text{------------------------------------} 2.44$$

Where,

q = Excess runoff in m^3/s

Pe = Excess rainfall in mm/hr

A = Catchment area in km^2

P_{net} (excess rainfall) was calculated as a depth in mm of the direct runoff (m^3) distributed uniformly over the whole catchment (divide volume by catchment area). This was used to establish a phi-index (Φ-Index) using an iterative method as was used by Sharma, such that the area under the Total Rainfall Hyetograph (TRH) above this index will be equal to P_{net} converted to the units of mm (Sharma, 1999). The portion of the TRH above this index will be extracted to give the Excess Rainfall Hyetograph (ERH). The established relationship between the excess rainfall and mobilized sediment was used to convert the ERH into a mobilized sediment histogram.

3.0 CHAPTER THREE: METHODOLOGY

3.1THE STUDY DATA

3.1.1 Data Required

The gist of this study is to model sediment transport in the upper Athi-River. The following data is required in order to undertake this study; rainfall intensities, suspended sediment data runoff discharge and area maps. These data must correspond to the study period. However, continuous recording of suspended sediment is only available for the period 1980 – 1981.Thus the available data limits the study to this period. The data was obtained from the Ministry of Water Development that gauged the river sediment during this period. The rainfall intensity data for the catchment was obtained from the Meteorological Department in Nairobi.

3.1.2 Quality Assurance on Data

These data were first subjected to quality assurance tests. The suspended sediment and runoff discharge were filtered of the extreme values that could affect the overall deterministic model, which is best used to forecast the average and not the extreme events.

The statistical tests used assumed that the data being tested is a sample from a single population (homogeneous sample). The statistical tests were done to uncover any heterogeneity in the data. This statistical investigation was also used to detect errors caused by changes of site, exposure and type of rain gauges used. Such changes can make the observations before and after the changes incomparable. It was therefore, important to examine the quality of the data that was used. Homogeneity tests based on the Cumulative Frequency Distributions (CFD) as developed by Haan and Bartlett were applied (Haan, 1977 and Bartlett, 1955).

The quality of the suspended sediment and runoff discharge data was checked using the co-efficient of correlation (r). A high value of r implies good correlation. Rainfall data consistency was checked using the Mass Curve Technique. Olwero and Opere found good results when they used this method for consistency checks (Olwero, 1997 and Opere, 1996).This technique involves the plotting of a double graph of time series of cumulative values of the rainfall. For homogeneous records, cumulative values would cluster around a single line (Haan, 1977 and Bartlett, 1955). By going through this quality assurance, suspect rainfall data were identified, modified or discarded altogether so that they did not yield erroneous conclusions.

3.2 METHODS OF DATA ANALYSIS

3.2.1 Development of a Sediment Rating Equation

According to Dunne very little work has been done on sediment transport within Kenyan catchments (Dunne, 1979). He also observed that while many rivers in Kenya already have their discharge rating equations developed the sediment rating equations for most of the rivers in the country are lacking. This includes the upper Athi River, which is the subject of this study.

This study developed a sediment rating equation for this subcatchment using Equation 2.6. The parameters of this equation were established through a log – linear transformation of Equation 2.6 as explained in Equation 2.7.

3.2.2 Development of the Instantaneous Unit Sediment Graph (IUSG) Model

The gist of this study was to develop a deterministic model that can be used to forecast sediment transport. This model has been used so far to estimate runoff volume. Very little work has been done to apply this model to sediment estimation. In this country Gikonyo has used the model to forecast sediment yield in Mathare river catchment (Gikonyo, 1994). He found out that the model gives a reasonable result when compared to the Time Area Histogram.

The IUSG model that was developed is given in equation 2.22.
The derivation of this model is given in Appendix 1. The parameters n and k was calculated using Equation 2.39 and 2.41.

3.2.3 Forecasting Suspended Sediment Load

The volume of suspended sediment was forecast using the IUSG model developed as already explained. To forecast the sediment transport, the effective rainfall series of time duration T was multiplied through by TUSG. The effective rainfall series was delineated from the rainfall recorded using the Phi – Index (Φ- Index) as explained in section 2.3.9.

Sediment graphs for given rainfall events were regenerated by convolution of the IUSG and the mobilized sediment histogram by following the numerical convolution in Equation. 2.43 and as illustrated in Figure 3.1. The IUSG obtained was integrated to get the S curve, see Figure 3.2. This in turn was lagged to obtain the TUSG. TUSG is the mobilized sediment by rainfall excess at the intensity of (1/T) mm/hr for a duration of T hours such that R=1mm.

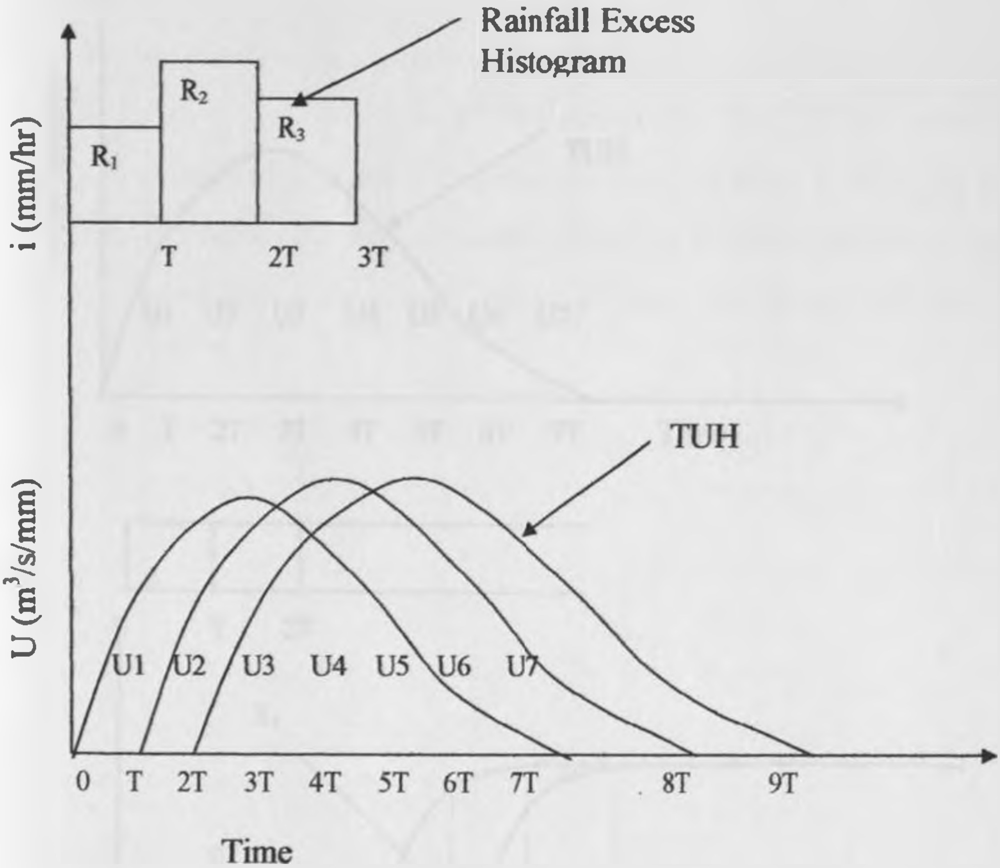

Figure 3.1: Illustration of Convolution Operation

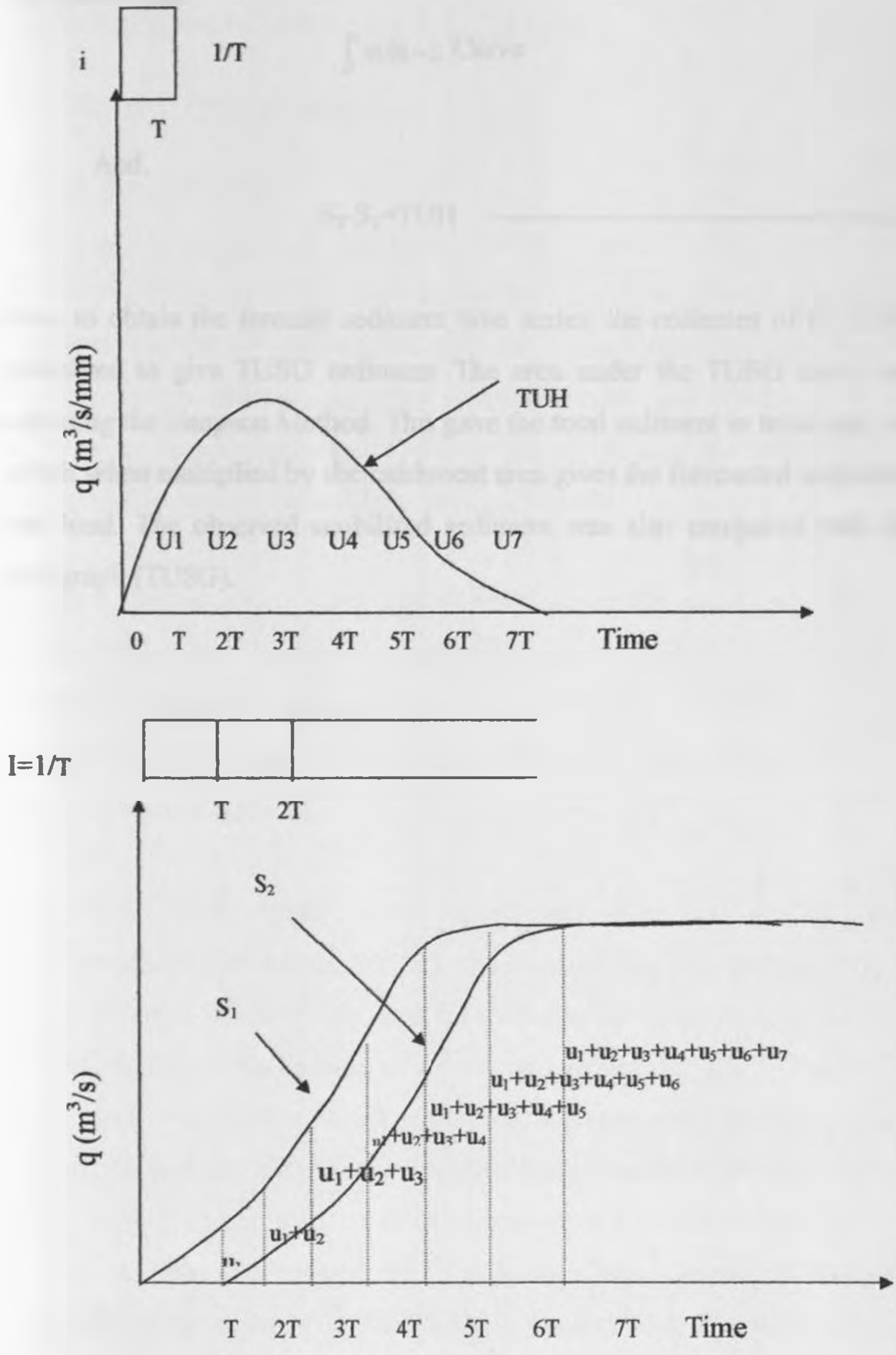

Figure 3.2: Illustration of "S" curve

In other words

$$\int_0^t IUH = S \text{ Curve}$$

And,

$$S_2 - S_1 = TUH \quad \text{------------------------------------} 3.1$$

Therefore, to obtain the forecast sediment time series, the ordinates of the IUSG was convolved to give TUSG ordinates. The area under the TUSG curve was obtained using the Simpson Method. This gave the total sediment in tones per unit area, which when multiplied by the catchment area gives the forecasted suspended sediment load. The observed mobilized sediment was also compared with the predicted graph (TUSG).

CHAPTER FOUR: RESULTS AND DISCUSSIONS

4.0 RESULTS AND DISCUSSIONS

4.1 Data Quality Assessment

It was necessary to perform an assessment of the quality of the rainfall and sediment data before it could be used to develop the IUSG model. This is a necessary procedure for all hydrological analysis because rainfall and sediment data could contain systematic errors. These systematic errors arise over a period of time due to many reasons including a shift in the location of the instrument, a change in type of the instrument and even in the personnel.

The data was first filtered to remove outliers. Outliers are data values that are not consistent with the other values, and which need to be removed from the analysis. The sediment and rainfall data values that were inconsistent with the rest of the data were identified and isolated using a graphical method. An example of these outliers can be seen in Figure 4.1.

Next it was necessary to check that the rainfall data to be used was of good quality. The consistency of the rainfall data was checked using the technique of a Simple Mass Curve, which is widely used for checking the consistency of rainfall data collected at many stations within or around the catchment of study. The Mass Curve Technique was applied to all the seven representative stations in the subcatchment. An example of how it was applied to one station is given in Figure 4.2. For this station all the data tends to cluster around a straight line, which indicates that the data is homogeneous. The Mass Curve Graphs for the six remaining rainfall stations showed a similar linear trend that had no breaks; hence the data are of good quality.

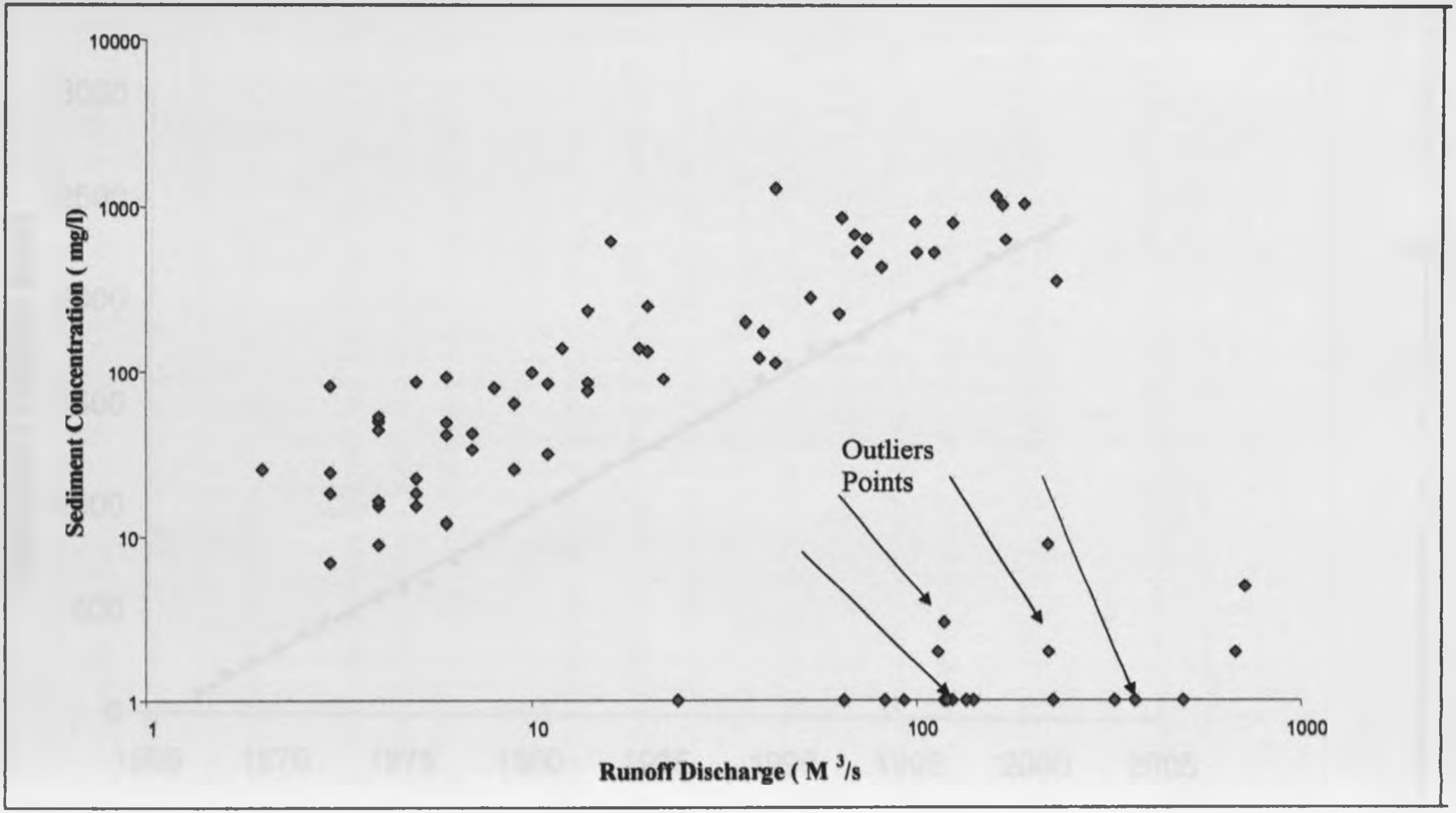

Figure 4.1: A Plot of Sediment Concentration against Runoff Discharge to Filter out the Outliers

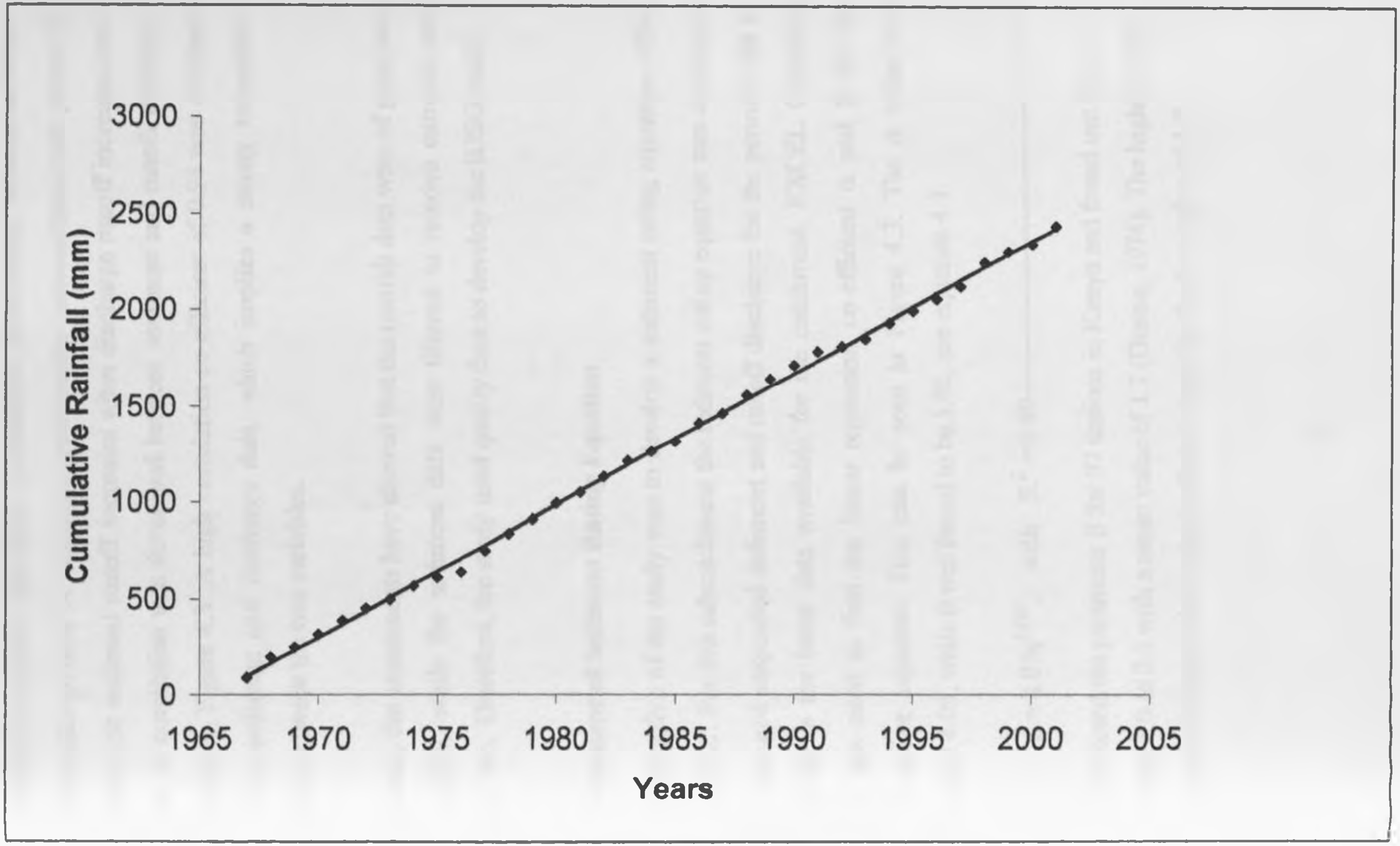

Figure 4.2: Mass Curve for Station Number 9136087

This technique has shown that the data does not contain systematic errors. Further, it was necessary to confirm that there is monotonic relationship between sediment and runoff discharge data. A monotonic relationship between these two pieces of data implies that sediment runoff increases when discharge runoff increases, and vice versa. A correlation was developed between sediment and runoff discharge data as given in Figure 4.3. A high correlation co-efficient of 0.94 was obtained between the sediment and discharge data, which implies a strong monotonic relationship between the two variables.

In conclusion, the assessments have showed that the rainfall data were of good and usable quality, while the sediment data were filtered to remove extreme and outlaying data. Therefore, the study used quality data to develop the IUSG model.

4.2 Development of Sediment Rating Equation

The first objective of the study was to develop a sediment rating equation of the form $C = \alpha q^{\beta} Z$. For this subcatchment the sediment rating equation was developed using the gauged suspended sediment and runoff discharge for the period 1980 to 1981, which is the latest data available for the catchment. EXCEL Computer Program was used to find the linear regression co-efficient α and β for the sediment rating equation. This can be seen in Figure 4.3. The α value was calculated as 4.05, while β was found to be 1.06, see equation 4.1.

$$C = 4.05q^{1.06}, \quad \text{with} \quad R^2 = 0.89 \qquad 4.1$$

Dunne calculated the parameter β for 97 stations in Kenya and found out that it ranged from 1.0 to 2.5 with a mean value of 1.7 (Dunne, 1974). The higher value of 2.5 is a non-conservative value and vice versa for the low value of 1.0.

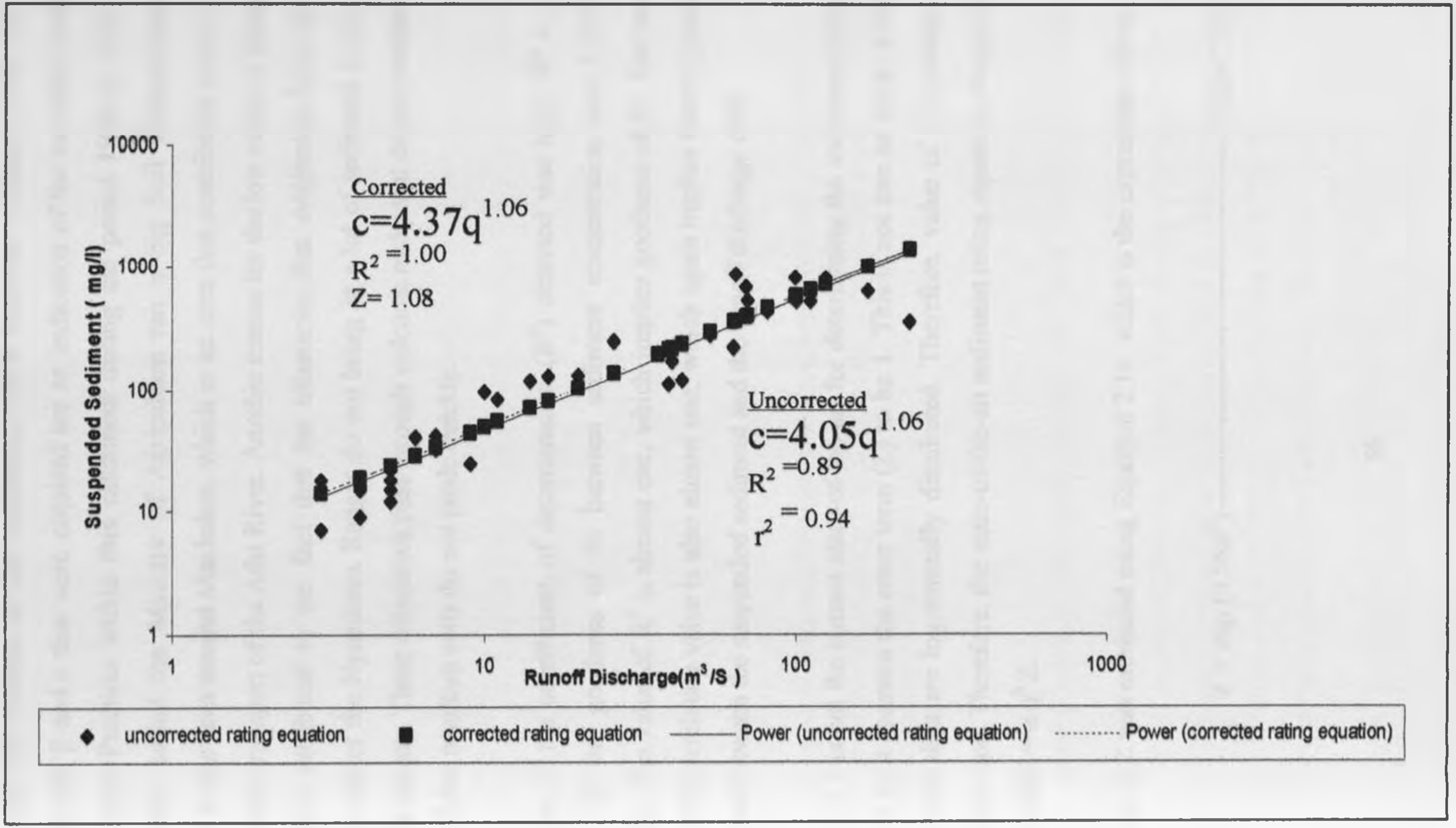

Figure 4.3: Sediment Rating Curve for Upper Athi River Catchment

For our rating equation, the parameter β value of 1.06 is low. A high value of β implies high soil erosion on the catchment, which increases sediment yield. The low values of β and α that were obtained are an indication of the extensive Soil Conservation Practices within this catchment during the period 1980 to 1981. During this period the Ministry of Agriculture ran a big Soil Conservation Program in the area around Machakos, which is an area that contributes much to the sediment transport of the Athi River. Another reason for the low value of β and α could be attributed to the fact that the tributaries that originates from the southern end of the Nyandarua Ranges do not bring in a lot of sediment for the following reason. These tributaries pass through volcanic rocks that do not weather easily and the resulting soils do not erode quickly.

The value of the co-efficient of determination (R^2) obtained was high. R^2 is a measure of the goodness of fit between sediment concentration and runoff discharge. The value of R^2 is almost one, which implies goodness of fit. The co-efficient of correlation value is also almost one, which again implies there is good correlation between the suspended sediment and the runoff discharge data.

Equation 4.1 is not the current state-of-the-art for determining the sediment rating equations as it assumes the error term (Z) to be 1. This is not true as most of the hydrological data are log-normally distributed. Therefore, value of Z is usually greater than one. Therefore, the state-of-the-art sediment rating equation should be of the form $C = \alpha q^{\beta} Z$.

The value of Z was estimated using Equation 2.18, which is the expression below,

$$Z = \exp(0.5Se^2) \text{ --------------------------------------- (Eqn 2.18)}$$

Again the EXCEL Computer Program was used to calculate the standard error of estimate (Se). This was found to be 0.39. Therefore, Se^2 becomes 0.152. From the expression above, this gives a Z value of 1.08. It is reasonable to conclude that our Z, which accounts for the errors present in the data, is plausible since its value is more than one. A Z value of one implies the absence of errors in the data. As discussed in section 4.1, our data were filtered of outliers to remove such errors.

The corrected equation, which is the state-of-the-art sediment rating equation then becomes,

$$C = 4.37q^{1.06} \quad ,\text{with} \quad R^2 = 1 \text{------------} 4.2$$

The value of R^2 and r are one for Equation 4.2. This implies a perfect fit since deviation errors have been cancelled out.

Equation 4.2 should be used for predicting catchment sediment yield because it takes into account the errors in the data.

4.3 Development of the Instantaneous Unit Sediment Graph (IUSG) Model

The second objective of the study is to develop the IUSG model using the rainfall, runoff and suspended sediment data.

4.3.1 Rainfall Data

The rain gauges measure the point rainfall. In future direct aerial rainfall measurements may be made by radar. In order to determine average rainfall over the subcatchment, seven representative stations were chosen and the technique of the Thiessen Polygon Method (Figure 4.4) was applied to estimate aerial rainfall. The rainfall measurements at individual gauges are first weighted by the fraction of the catchment represented by the gauges and then summed. On the map of the catchment, the rain gauge stations are plotted using the grid locations, the catchment area is divided into polygons by lines that are equidistant for well distributed gauges as shown in Fig 4.4. The polygon area a_i corresponding to the rain gauge station is calculated and the aerial rainfall given by,

$$\overline{R} = \frac{\sum_{i=1}^{n} R_i a_i}{\sum_{i=1}^{n} a_i} = \frac{\sum_{i=1}^{n} R_i a_i}{A} \quad \text{------------------------------} 4.3$$

Where a_i/A is the aerial function called the Thiessen Co-efficient, which represent the weighting factors.

Since the map was drawn to scale, the polygon areas for the seven stations were calculated using the graphical method. That is, the map was traced on a graph paper and by using the scale of the map, one square represented 100 Km^2. The areas are given in Table 4.1.

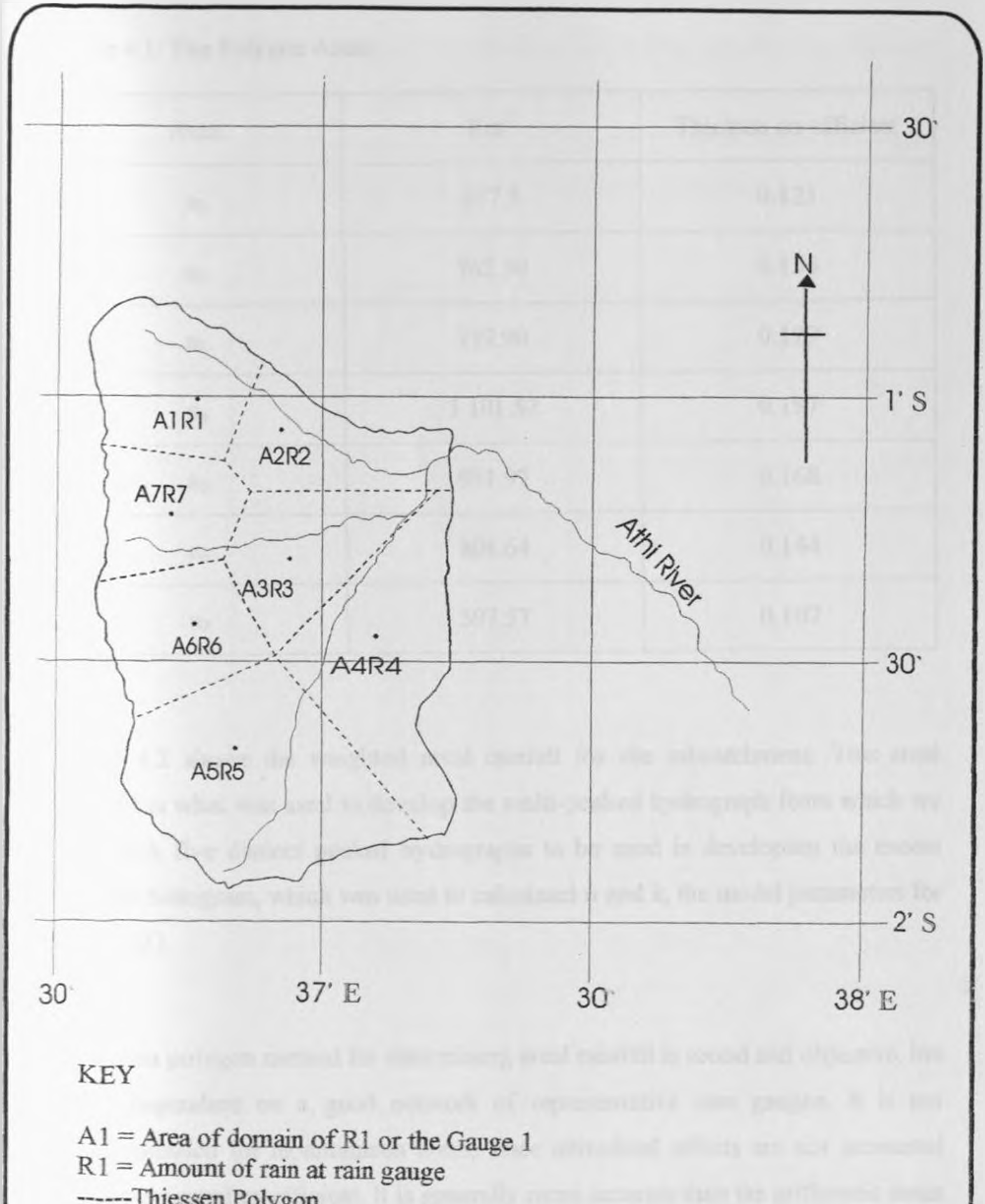

Figure 4.4: Thiessen Polygons for the Subcatchment

Table 4.1: The Polygon Areas

Area	Km^2	Thiessen co-efficient
a_1	677.5	0.121
a_2	762.30	0.136
a_3	719.90	0.129
a_4	1 101.52	0.197
a_5	931.97	0.168
a_6	804.64	0.144
a_7	597.57	0.107

Table 4.2 shows the weighted areal rainfall for the subcatchment. This areal rainfall is what was used to develop the multi-peaked hydrograph from which we will pick five distinct peaked hydrographs to be used in developing the excess rainfall histogram, which was used to calculated n and k, the model parameters for the IUSG.

Thiessen polygon method for determining areal rainfall is sound and objective, but it is dependent on a good network of representative rain gauges. It is not recommended for mountainous areas, since altitudinal effects are not accounted for by the areal co-efficient. It is generally more accurate than the arithmetic mean method, but it is inflexible as a new Thiessen network must be constructed each time there is a change in the gauge network or location.

It is well recognized that UH is an important tool for flood synthesis of the flood hydrographs. It is, therefore, necessary that the UH for a catchment must be known beforehand. It is derived using the rainfall and runoff information for the gauged catchments. The derivation is simple for the single peaked storm.

Table 4.2: Study Catchment Average Areal Rainfall Intensities (mm/hr)

Months / Days	Jan	Feb	Mar	Apr	May	Jun	Jul	Aug	Sept	Oct	Nov	Dec
1		0.51	1.94		5.33						0.68	
2			1.59		4.56						0.28	
3			1		2.39						2.42	
4					3.1				0.12		1.54	
5					4.09						4.37	2.06
6					2.35	0.41		0.16		0.68	0.20	0.43
7			0.36	0.38	5.83	0.34		0.46			2.64	1.06
8				3.68	1.59		0.12	1.76		3.25	1.67	1.5
9				5.49	2.06		0.20	0.04			2.69	
10									0.12			
11				1.6	4.75						2.53	
12				2.06	4.57			1.51		2.26		0.18
13				3.59	5.06			0.79		1.6	0.56	1.82
14		1.17		2.96	1.19				1.87	0.88	3.4	
15				1.22	2.18						4.93	

Table 4.2: Study Catchment Average Areal Rainfall Intensities (mm/hr) (Continuation)

Months / Days	Jan	Feb	Mar	Apr	May	Jun	Jul	Aug	Sept	Oct	Nov	Dec
16				2.96	0.77			0.06			2.08	
17				1.46	7.36						3	2.16
18				3.85	1.02					0.29	1.21	2.11
19				2.33				1.73		0.25	4.4	
20				4.25							0.27	
21				2.93			0.03				3.74	
22				1.71	4.06	0.28					1.09	
23				4.12	1.72	6.62		0.22	0.59		1.31	
24	1.9		2.68	8.9	0.04			0.48	0.45		1.37	
25			0.52	1.97	0.11	0.31		0.01			0.22	
26	4.41			1.05	1						1.26	
27	1.2									0.23	2.2	
28			2.34				0.25			0.99	0.64	
29	1.23	0.38	3.41		6.72	1.38				0.3		
30	0.98		2.49		1.8	0.89						
31	2.02		0.72									

But very often, particularly on large catchments, like in our case, it is difficult to find in the available records enough single peaked storms. Multiple peaked sequences of rainfall and runoff hydrographs are then analyzed to derive the Unit

Hydrographs (Figure 4.5 and 4.6). In Figure 4.5, it was impossible to find days without rainfall because it represent the average areal rainfall for the entire catchment. That is, if it is not raining on one part, then there is rain on the other part of the catchment during the rainy season.

The analysis of the multiple peaked sequences of rainfall hyetographs and runoff hydrographs starts with the identification of at least five distinct peaked hydrographs and the corresponding hyetographs, Figure 4.5 and 4.6. For the identified runoff hydrographs, the storm duration should be equal or within 25%. For the identified runoff hydrograph, the hydrograph was separated for both direct runoff and base flow using a straight line method.

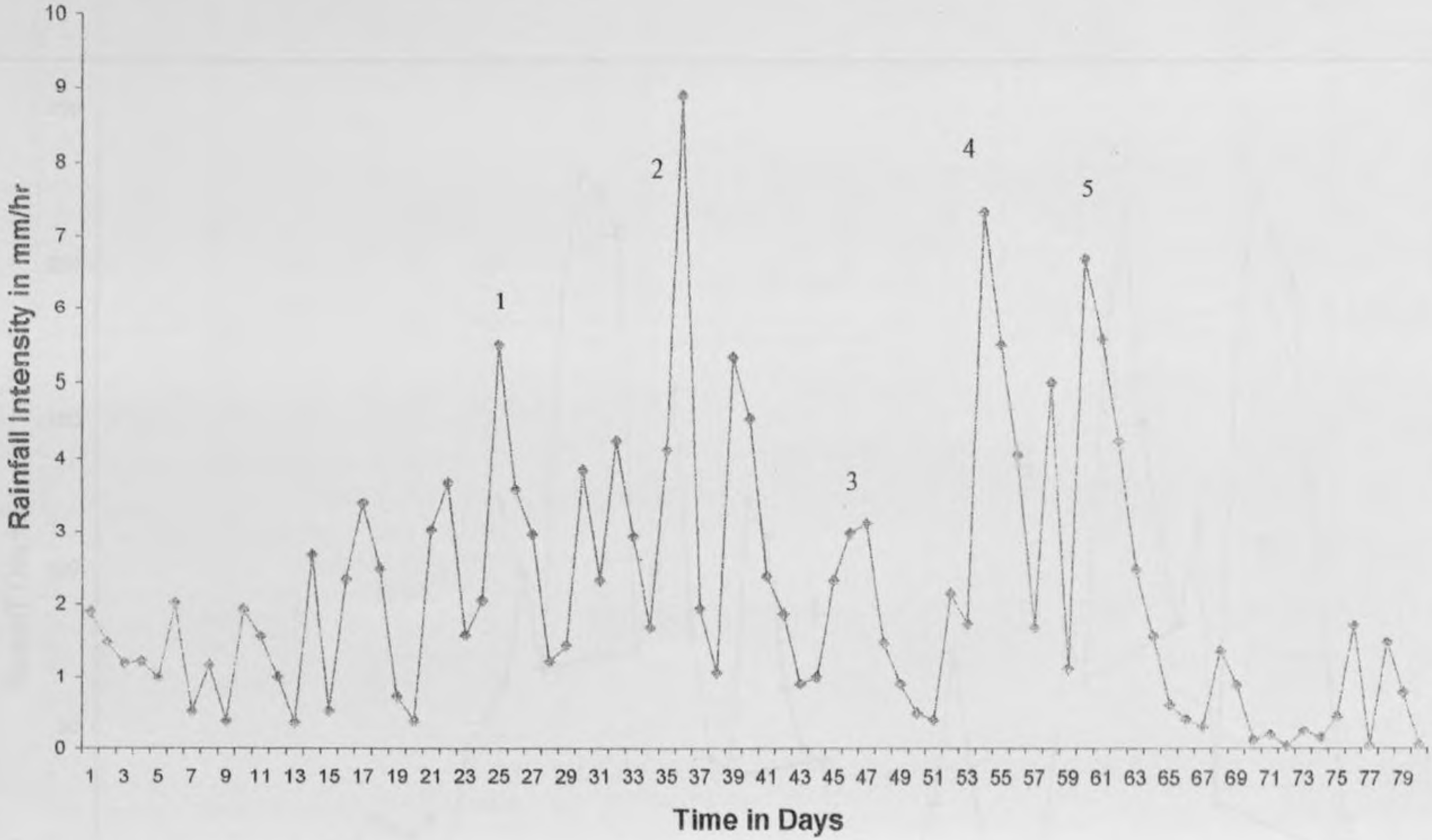

Key: 1,2,3,4 &5 are the rainfall extracted for the study

Figure 4.5: Rainfall Multi-Peaked Sequence Hydrographs for the Subcatchment

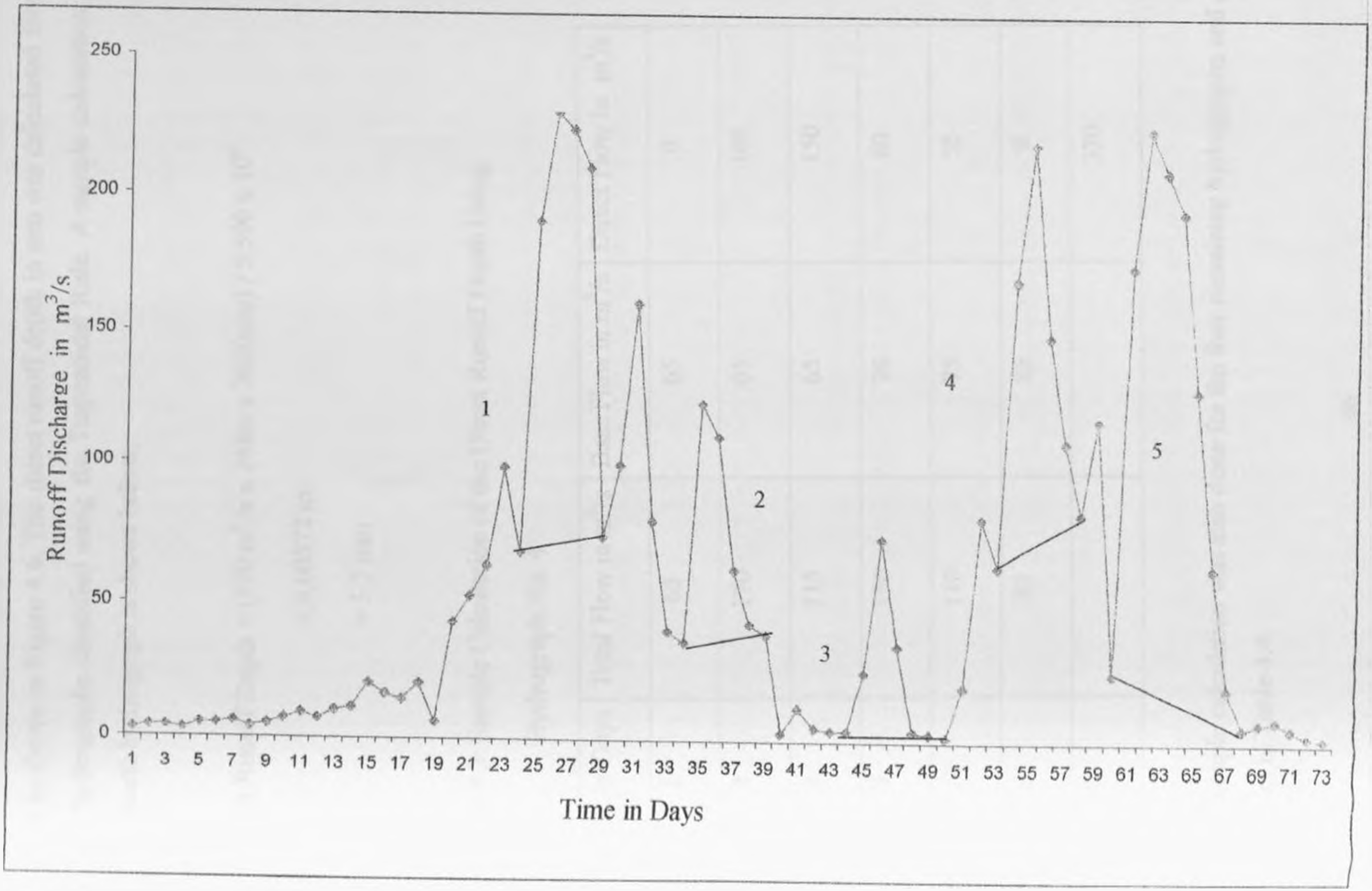

Figure 4.6: Runoff [illegible]

This was done by drawing a tangent to the curve between the falling and the rising limb as shown in Figure 4.6. The direct runoff depth in mm was calculated for the five hydrographs identified using the Trapezoidal Rule. A sample calculation for the fourth hydrograph is shown below,

Direct Runoff Depth = (370 m^3/s x 24hrs x 3600sec) / 5 590 x 10^6

= 0.00572 m

= 5.7 mm

Table 4.3: Sample Calculation of the Direct Runoff Depth Using Hydrograph No. 4

Time in Days	Total Flow in m^3/s	Base Flow in m^3/s	Direct Flow in m^3/s
1	65	65	0
2	170	65	105
3	215	65	150
4	150	70	80
5	110	75	35
6	85	85	0
			370

The sample calculation was also done for the four remaining hydrographs and can be seen in Table 4.4.

Table 4.4: Direct Runoff Depth for the Five Identified hydrographs

Hydrographs	Direct Runoff Depth in mm
1	8.8
2	4.9
3	3.95
4	5.7
5	11.7

The direct runoff together with the identified rainfall hyetographs was used to calculate the rainfall excess through using the Φ -index procedure. The Φ-index for both the five hydrographs was calculated using the iterative method.

The excess rainfall obtained was turned into Excess Runoff Volume using Equation 2.44. Both the Excess Runoff volume and the Direct Runoff were used to construct the Histogram, which was used to calculate the parameters n and k using the method of moments as discussed in the succeeding section.

A relationship was also derived between Excess Runoff and Mobilized Sediment using linear regression in the EXCEL Computer Program. The relationship obtained is as shown in equation below,

$$S_m = 2.05Pe^{0.62} \text{ With } R^2 = 0.82 \text{and } r = 0.91 \text{-----------------} 4.4$$

Where,

S_m = Mobilized sediment in t/day

Pe = Excess runoff in mm

The values of R^2 and r obtained are high, which clearly indicates a perfect fit and a good correlation between mobilized sediment and rainfall excess.

4.3.2 Evaluation of the Parameters n and k

The parameters n and k are calculated by determining the moments of the Excess Rainfall Hyetograph (ERH) and the Direct Runoff Hydrograph (DRH) as explained in section 2.3.8. Each block in the ERH and DRH has duration of 24 hours. The rainfall excess has been converted to units of m^3 /s by multiplying by the catchment area using Equation 4.4 to be dimensionally consistent with the runoff.

A sample calculation has been done on Hydrograph No. 4 to show how ***n*** and ***k*** are obtained. The procedure is outlined below.

From Figure 4.5, the rainfall hyetograph for the hydrograph being used was extracted and can be seen in Figure 4.7,

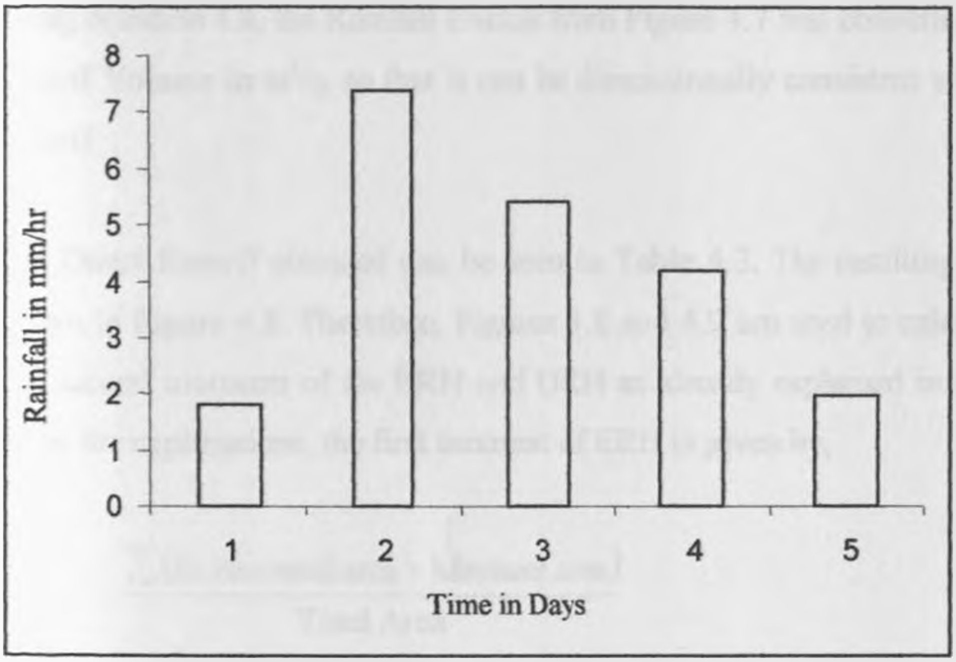

Figure 4.7: Rainfall Hyetograph for Hydrograph No. 4

From the sample calculation of Direct Runoff Depth (DRD) for the fourth hydrograph in Table 4.4, the DRD was calculated to be 5.7 mm. This runoff depth is the rainfall excess. Therefore, using the iterative method on Figure 4.7, The Φ - index was obtained to be 3.75 mm/hr. This gives rainfall excess of 3.65, 1.65 and 0.45 mm for the chosen hydrograph. The iterative method of obtaining the Phi-index was performed on the remaining hydrographs and the results are shown in Table 4.5.

Table 4.5: Φ – Index Values

Hydrographs	Φ – Index in mm/hr
1	1.45
2	4.05
3	1.55
4	3.75
5	1.75

Using equation 4.4, the Rainfall Excess from Figure 4.7 was converted into Excess Runoff Volume in m^3/s, so that it can be dimensionally consistent with the Direct Runoff

The Direct Runoff obtained can be seen in Table 4.3. The resulting histogram is shown in Figure 4.8. Therefore, Figures 4.8 and 4.9 are used to calculate the first and second moments of the ERH and DRH as already explained in section 2.3 8. From the explanations, the first moment of ERH is given by,

$$ML_1 = \frac{\sum(\text{Incremental area} \times \text{Moment arm})}{\text{Total Area}}$$

$$= \frac{1}{9224.89}(5855.80 \times 12 \quad + \quad 2647.14 \times 36 \quad + \quad 721.95 \times 60) \text{-----------} 4.5$$

$$ML_1 = 22.64 \text{ hr}$$

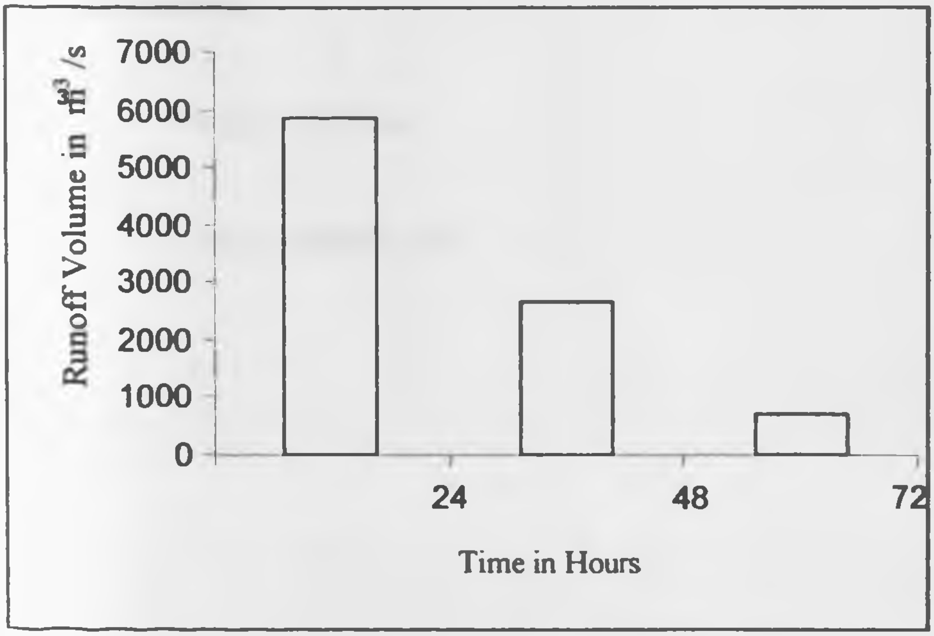

Figure 4.8: Excess Runoff Histogram

The second moment of ERH is given by,

$$ML_1 = \frac{\Sigma\left(A \times (B)^2\right) + \Sigma(C)}{\text{Total Area}}$$

$$ML = \frac{1}{9224.89}\left(5855.80 \times 12^2 + 2647.14 \times 36^2 + 721.95 \times 60^2\right) + \frac{1}{12} \cdot 24^2 (9224.89) \quad \text{—4.6}$$

$$ML_1 = 793.04 \text{ hr}^2$$

Where,

A = Incremental area

B = Moment arm

C = Second moment about centroid of each increment

By a similar calculation for the DRH in Figure 4.9, the first and second moments for runoff becomes,

$MQ_1 = 38.92$ hr

And,

$MQ_2 = 2060.11$ hr^2

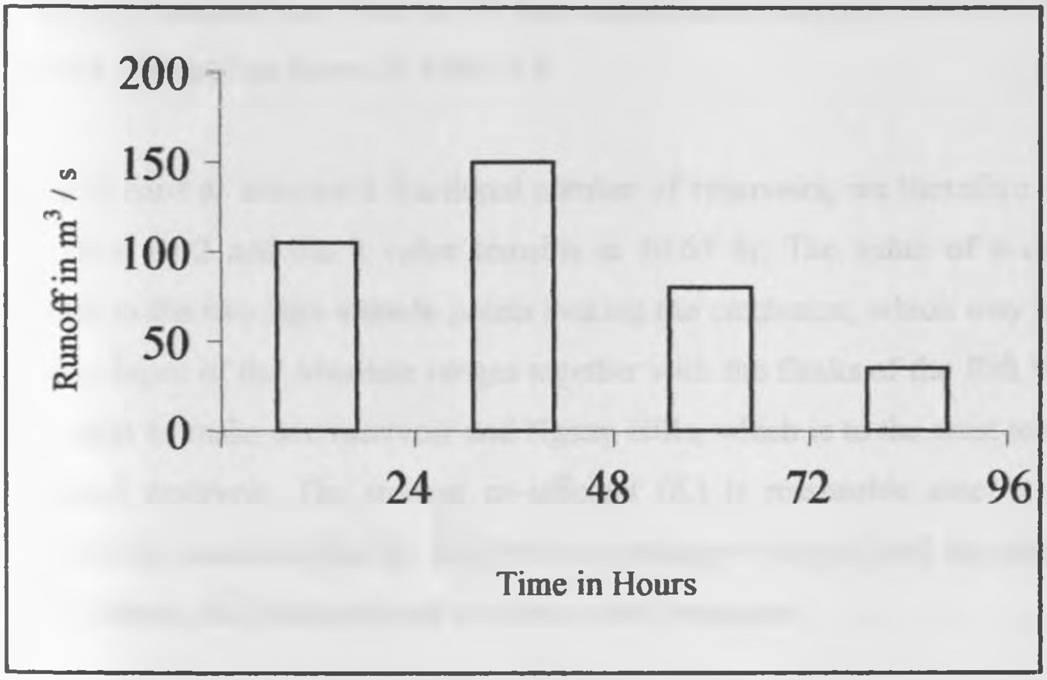

Figure 4.9: Direct Runoff Histogram

Therefore, using Equation 2.39 and 2.41 in section 2.3.8, we then calculate the value of n and k as,

$$MQ_1 - ML_1 = nk \text{------------------------------} \text{----------- (Eqn 2.39)}$$

$$38.92 - 22.64 = 16.28 \text{ hr} = nk$$

Likewise,

$$MQ_2 - ML_2 = n^2k^2 + nk^2 + 2nkML_1 \text{------------------ (Eqn 2.41)}$$

$$= (nk)^2 + (nk)\,k + 2\,(nk)\,ML_1$$

$$2060.11 - 793.04 = 16.282 + 16.28k + 2 \times 16.28 \times 22.64$$

$$1267.07 - 1002.2 = 16.28k$$

$$k = 16.27$$

If nk is equal to 16.28 and k is equal to 16.27, then

$$n = 16.28/16.27$$

$$= 1$$

Therefore, the values of n and k are 1 and 16.27.

The above procedure was done on the four remaining hydrographs and the values of n and k obtained as shown in Table 4.6.

Since it is hard to imagine a fractional number of reservoirs, we therefore round the n value to 2 and the k value remains at 10.61 hr. The value of n can be attributed to the two high altitude points making the catchment, which may be the southern slopes of the Aberdare ranges together with the flanks of the Rift Valley to the south to make one reservoir and Ngong Hills, which is to the west to make the second reservoir. The storage co-efficient (K) is reasonable since a good percent of the catchment had by this time not undergone serious land use changes, as most farmers had instituted soil erosion control measures.

Table 4.6: Values of n and k for the Five Hydrographs

Hydrographs	n	k
1	1.51	10.59
2	1.77	9.85
3	2.19	8.68
4	1.00	16.27
5	2.49	7.64
Average	1.79 = 2.00	10.61

4.3.3 Development of the Nash Model

The average values of n and k for the entire subcatchment were used to develop the IUSG model. The values were substituted in the expression below to give the ordinates of the IUH. The ordinates computed can be partly seen in Table 4.7, and the rest are placed in appendix 2.

$$u(t) = \frac{1}{k\Gamma n}\left(\frac{t}{k}\right)^{n-1} e^{\frac{-t}{k}} \text{ ---------------------------- (Eqn 2.22)}$$

The resultant hydrograph (Fig 4.10) is the Instantaneous Unit Hydrograph (IUH). Therefore, to obtain the IUSG model, the IUH ordinates were substituted in the current state-of-the-art sediment rating equation below,

$$C = 4.37q^{1.06} \text{ ------------------------------------- (Eqn 4.2)}$$

The results gave the ordinates of the IUSG model developed; these ordinates can also be seen in Table 4.7. Figure 4.11 then becomes the IUSG model developed, which will be convolved with the mobilized sediment for the forecasting of the suspended sediment load in the section below.

Table 4.7: The Ordinates of the IUH and IUSG Model Developed (The full table of values is given in Appendix 2)

Time in Days	$\frac{1}{k\Gamma n}$	$e^{\frac{-t}{k}}$	$\left(\frac{t}{k}\right)^{n-1}$	U (t) m^3/hr	IUH U (t) m^3/day	IUSG t/day
0	0.091	1	0	0	0	0
1	0.091	0.910	0.082	0.00679	0.163	0.64
2	0.091	0.829	0.170	0.013	0.308	1.25
3	0.091	0.754	0.261	0.018	0.430	1.79
4	0.091	0.687	0.355	0.022	0.533	2.24
5	0.091	0.625	0.449	0.026	0.613	2.60
6	0.091	0.569	0.545	0.028	0.677	2.89
7	0.091	0.518	0.642	0.030	0.726	3.11
8	0.091	0.471	0.739	0.032	0.760	3.27

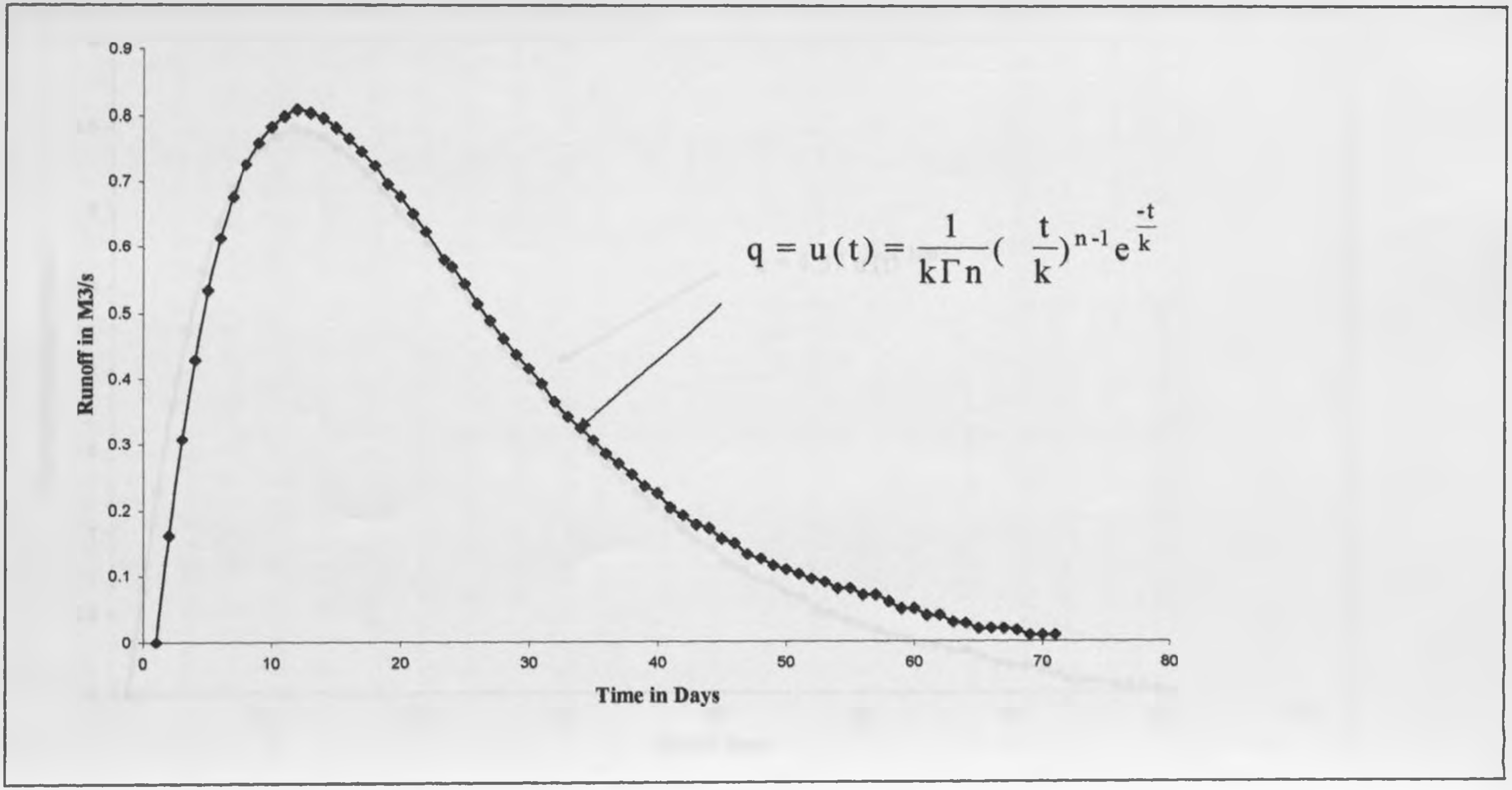

Figure 4.10: Instantaneous Unit hydrograph for the Upper Athi River Subcatchment

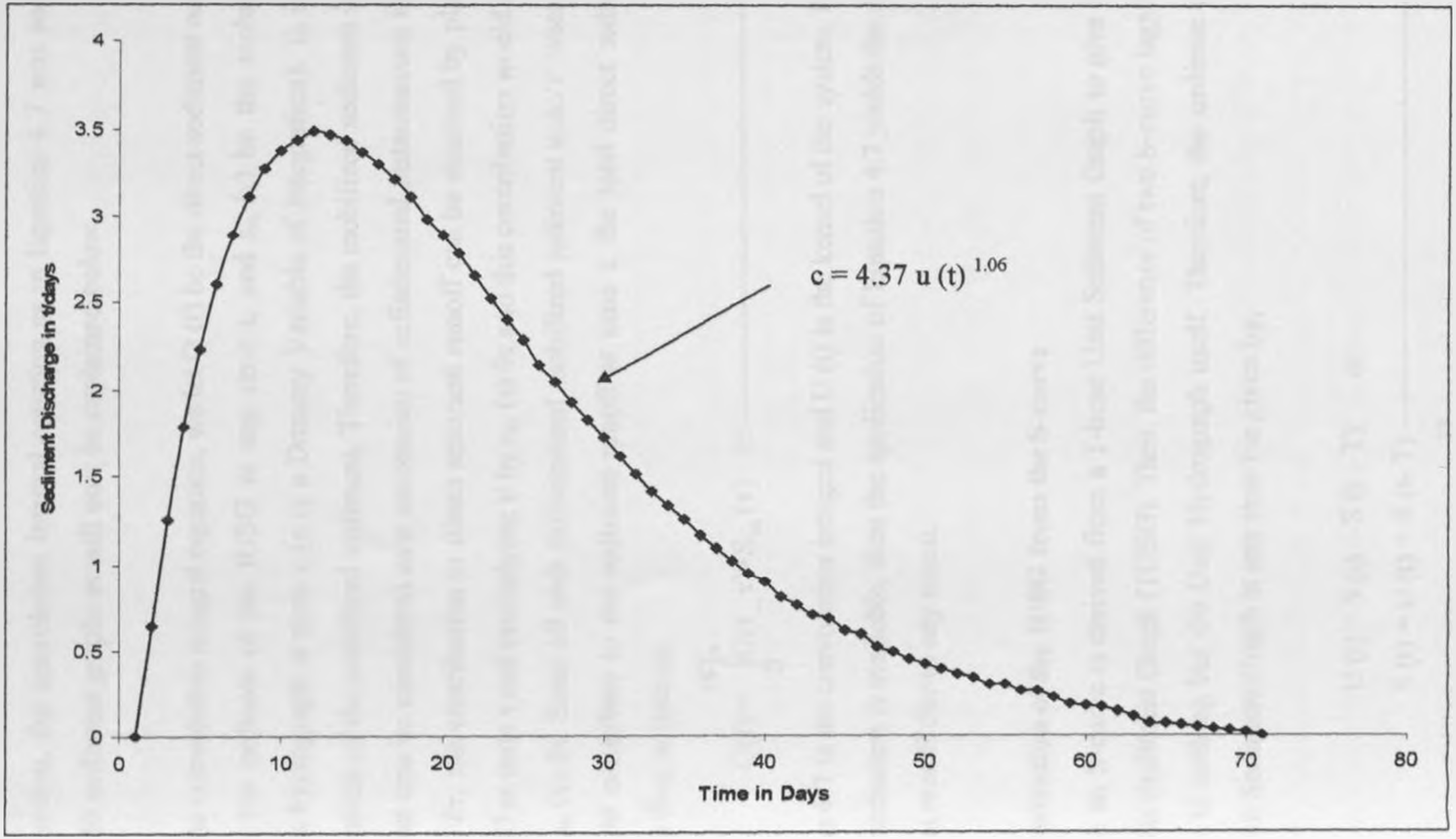

Figure 4.11: Instantaneous Unit Sediment Graph (IUSG) Model

4.3 Forecasting the Suspended Sediment Using the IUSG Model

In this section, the convolution integral equation as in Equation 4.7 was used to predict the sediment graphs as will now be explained below.

To get the convolution integral equation, we let Q (t) be the direct sediment runoff, u (t) be the ordinate of the IUSG at any time t, and s_m (τ) be the mobilized sediment hyetograph at time τ (τ is a Dummy Variable of Integration). T_0 is the total duration of the mobilized sediment. Therefore, the mobilized sediment in the catchment can be considered as a succession of infinitesimal instantaneous inputs of s_m (τ) $\delta\tau$, the contribution to direct sediment runoff can be obtained by placing the IUSG at time τ and multiplying it by s_m (τ) $\delta\tau$ and this contribution would be U (t – τ). s_m (τ) $\delta\tau$. Since all such infinitesimal mobilized sediment upto't' where t $\leq$ T_o, would contribute to the sediment runoff at time t, the total direct sediment runoff is thus written as,

$$Q(t) = \int_0^{t \le T_0} U(t\_\tau) \bullet S_m(\tau) \ \partial\tau \text{ --------------------------------------- } 4.7$$

Equation 4.7 is the convolution integral and U (t) is the kernel of the system. IUSG of the catchment is available, then the application of Equation 4.7 yields the direct sediment runoff due to any storm.

4.4.1 Derivation of the IUSG from the S-curve

Suppose an S-curve is derived from a T-hour Unit Sediment Graph to give the t-hour Unit Sediment Graph (TUSG). Then, the difference of two S-curve lagged by T-hours is nothing but the Unit Hydrograph itself. Therefore, the ordinate of T-hour Unit Sediment Graph at any time t is given by,

$$U(t) = S(t) - S(t-T) \quad \text{or}$$

$$S(t) = U(t) + S(t-T) \text{ --- } 4.8$$

Thus the ordinate of the S-curve at any time t is obtained as the sum of the unit hydrograph ordinates at t and the S-curve addition, where the S-curve addition is also an ordinate of S-curve itself but at time (t –T). For $t \leq T$, the ordinates of the S-curve T-hour USG are identical. For $t > T$, Equation 4.8 provides an easy way of constructing the S-curve.

If an S-curve hydrograph is derived from an available unit hydrograph of duration t hr, and U (t, Δt) denotes the ordinates of Δt hour unit hydrograph at any time 't', then, from S-curve technique in Equation 4.8, we have,

$$U(t, \Delta t) = \Delta / \Delta t\,(S(t) - S(t - \Delta t)) = T.\ \Delta S(t) / \Delta t)$$

Where,

S (t) is the S-curve ordinate. In the limit as $\Delta t \rightarrow 0$, we get the IUSG as,

$$\lim_{\Delta t \rightarrow 0} U(t, \Delta t) = U(t) = T.\ (t)\ ds / dt$$

Therefore,

$$U(t) = T.\ ds(t) / dt \text{--} 4.9$$

In other words, the ordinate of IUSG at any time t is equal to T * (The slope of the S-curve derived from T hour unit hydrograph at t). Since the S-curve hydrograph derived from a TUSG cannot be too exact, the IUSG obtained from this method is only approximate.

4.4.2 Derivation of a TUSG from the IUSG Model

As given by the convolution integral, the direct sediment runoff is expressed as given in Equation 4.7. If we consider the input rainfall of intensity 1/ T mm/hr for an infinite duration, the corresponding output runoff is nothing but the S-curve hydrograph. So replacing Q (t) by S (t) and s_m (t) by (1/ T) in equation 4.7, we get,

$$S(t)=\frac{1}{T}\int_{0}^{t} U(t-\tau)\ \partial\tau \qquad \text{4.10}$$

By introducing the transformation that z = (t-T) in the above integral, then we have, $\delta\tau = -\delta z$, and the limits, when $\tau = 0$ when z = t and $\tau = t$ when z = 0. Equation 4.10 now becomes,

$$S(t)=\frac{1}{T}\int_{t}^{0} U(z)(-dz)=\frac{1}{T}\int_{0}^{t} U(z).dz \qquad \text{4.11}$$

$$S(t)=\frac{1}{T}\int_{0}^{t} U(z).dz$$

So the ordinates of S-curve at time t, resulting from an infinite rainfall of intensity 1/ T mm/hr can be obtained as 1/ T x (The integration of IUSG from 0 to t). Conversely, the ordinates of IUSG at time t may be obtained as T * (The differential of the S-curve at t). That is,

$$U(t) = T.\ ds(t) / dt$$

Now let U (t, T) be the ordinate of TUSG at time t and let S (t) be the S-curve obtained from this TUSG. Then from Equation 4.8 we have,

$$U(t,T)=S(t)-S(t-T)$$

$$=\frac{1}{T}\int_{0}^{t} U(z)dz-\frac{1}{T}\int_{0}^{t-T} U(z)dz$$

$$U(t,T)=\frac{1}{T}\int_{t-T}^{t} U(z)dz \qquad \text{4.12}$$

That means that the ordinates of the TUSG at t = (1/ T x (The area of IUSG in the limits between (t – T), and t)).

If the IUSG is assumed to be linear between (t – T) and t, then Equation 4.12 becomes

$$U(t, T) = U(t - T/2) \text{ -- } 4.13$$

However, it is to be noted that Equation 4.13 works well only when T is small and when the peak is not contained within the interval (t – T) to t. Equation 4.12 can be used to derive the TUSG of any duration T, provided the IUSG is available, thus eliminating the construction of the S-curve hydrograph.

4.4.2 Sample Calculation of the TUSG Ordinates Using the Convolution Integral Equation

In this part, a sample calculation on how to get the ordinates of the T-hour USG (TUSG) using Equation 4.12 is given. T is taken as one day. The ordinates of the TUSG are as given in Table 4.8. To derive the ordinates of the 1 day USG from this ISUG the following procedure was used. For each of the 1 day USG, integrate the IUSG between t – T and t, and divide by T. For example, the ordinate of 1 day USG at the 10 day is given by,

For the 10th day, our t = 10 and T =1, therefore, the ordinate is given by,

10th day ordinate = 1 / T (area of IUSG between (t – T) day and t day)

= 1 / 1 (area of IUSG between (10 – 1) and 10th day)

= 1/ 1 (area of IUSG between 9th day and 10th).

Assuming the variation of IUSG is approximately linear between the 9th and 10th day, then the ordinate of 1 day USG on the 10th day is given by,

= 1 / 1 ((ordinate of IUSG at 9th day + ordinate of IUSG at 10th day) x 1) / 2

= (3.38 + 3.44)/ 2

= 3.41.

Similarly all other ordinates of TUSG are computed and entered in Table 4.8 below.

Table 4.8: IUSG and TUSG Ordinates

Days	IUSG Tonnes/day	TUSG Tonnes/day	Days	IUSG Tonnes/day	TUSG Tonnes/day
0	0	0	36	1.09	1.13
1	0.64	0.32	37	1.20	1.06
2	1.25	0.95	38	0.95	0.99
3	1.79	1.52	39	0.90	0.93
4	2.24	2.02	40	0.81	0.86
5	2.60	2.42	41	0.76	0.79
6	2.89	2.75	42	0.70	0.73
7	3.11	3.00	43	0.68	0.69
8	3.27	3.19	44	0.61	0.65
9	3.38	3.33	45	0.59	0.60
10	3.44	3.41	46	0.52	0.56
11	3.49	3.47	47	0.49	0.51
12	3.47	3.48	48	0.45	0.47
13	3.44	3.46	49	0.42	0.44
14	3.37	3.41	50	0.39	0.41
15	3.30	3.34	51	0.36	0.38
16	3.21	3.26	52	0.34	0.35
17	3.11	3.16	53	0.30	0.32
18	2.98	3.00	54	0.30	0.30
19	2.89	2.94	55	0.26	0.28
20	2.78	2.84	56	0.26	0.26
21	2.65	2.72	57	0.22	0.24

Table 4.8: IUSG and TUSG Ordinates

Days	IUSG Tonnes/day	TUSG Tonnes/day	Days	IUSG Tonnes/day	TUSG Tonnes/day
22	2.52	2.59	58	0.18	0.2
23	2.40	2.46	59	0.17	0.18
24	2.29	2.35	60	0.16	0.17
25	2.15	2.22	61	0.14	0.15
26	2.05	2.1	62	0.11	0.13
27	1.93	1.99	63	0.07	0.09
28	1.83	1.88	64	0.07	0.07
29	1.73	2.7	65	0.06	0.07
30	1.62	1.68	66	0.05	0.06
31	1.51	1.57	67	0.04	0.05
32	1.41	1.46	68	0.03	0.04
33	1.33	1.37	69	0.02	0.03
34	1.25	1.29	70	0.001	0.01
35	1.16	1.21			

The ordinates of the IUSG and TUSG were plotted together as shown in Figure 4.12. As expected, the rising limb of the IUSG is higher than the rising limb of the TUSG and vice-versa for the falling limb. This is because, for the IUSG, it is an instantaneous burst of one unit of mobilized sediment. So it is expected to rise first and fall first than the TUSG, with the peak also coming first.

4.4.3 Testing the Model

In this section, we are going to forecast the annual sediment yield from the catchment and also to compare the predicted and the observed sediment data.

The TUSG above was developed while assuming a rainfall intensity of 1 / T mm/hr, with T taken as one. Therefore, to get the sediment graph for the catchment that will be used in forecasting sediment, we use the average intensity in the catchment, which is 1.91 mm/hr, see Table 4.2. This average catchment intensity when multiplied with the TUSG ordinates will give the catchment sediment graph shown in Figure 4.13. Therefore, using Simpson's Method as in equation 4.14 on Figure 4.13, we get the catchment sediment in tonnes per unit area to be 187.95 t/km^2/yr. If we now consider the total area of the catchment, then we obtain the annual sediment yield to be 1.05 million tonnes. This translates to one eighth of the entire sediment yield monitored at Sabaki by Mansell- Moullin in 1973. The production rate then becomes 187.95 t/km^2/y as compared to the figure given by Wain in 1983 of 118 t/km^2/yr, when he used the flow duration – sediment rating curve.

$$\int_{Ymean}^{d} X\, dy = \frac{1}{3}\left[(W) + 4(Y) + 2(Z)\right] \quad \text{------------------------------} 4.14$$

Where,

$$W = \bar{X}_1 + \bar{X}_n$$

$$Y = \bar{X}_2 + \bar{X}_4 + \ldots\ldots\ldots\ldots + \bar{X}_{n-1}$$

$$Z = \bar{X}_3 + \bar{X}_5 + \ldots\ldots\ldots\ldots + \bar{X}_{n-2}$$

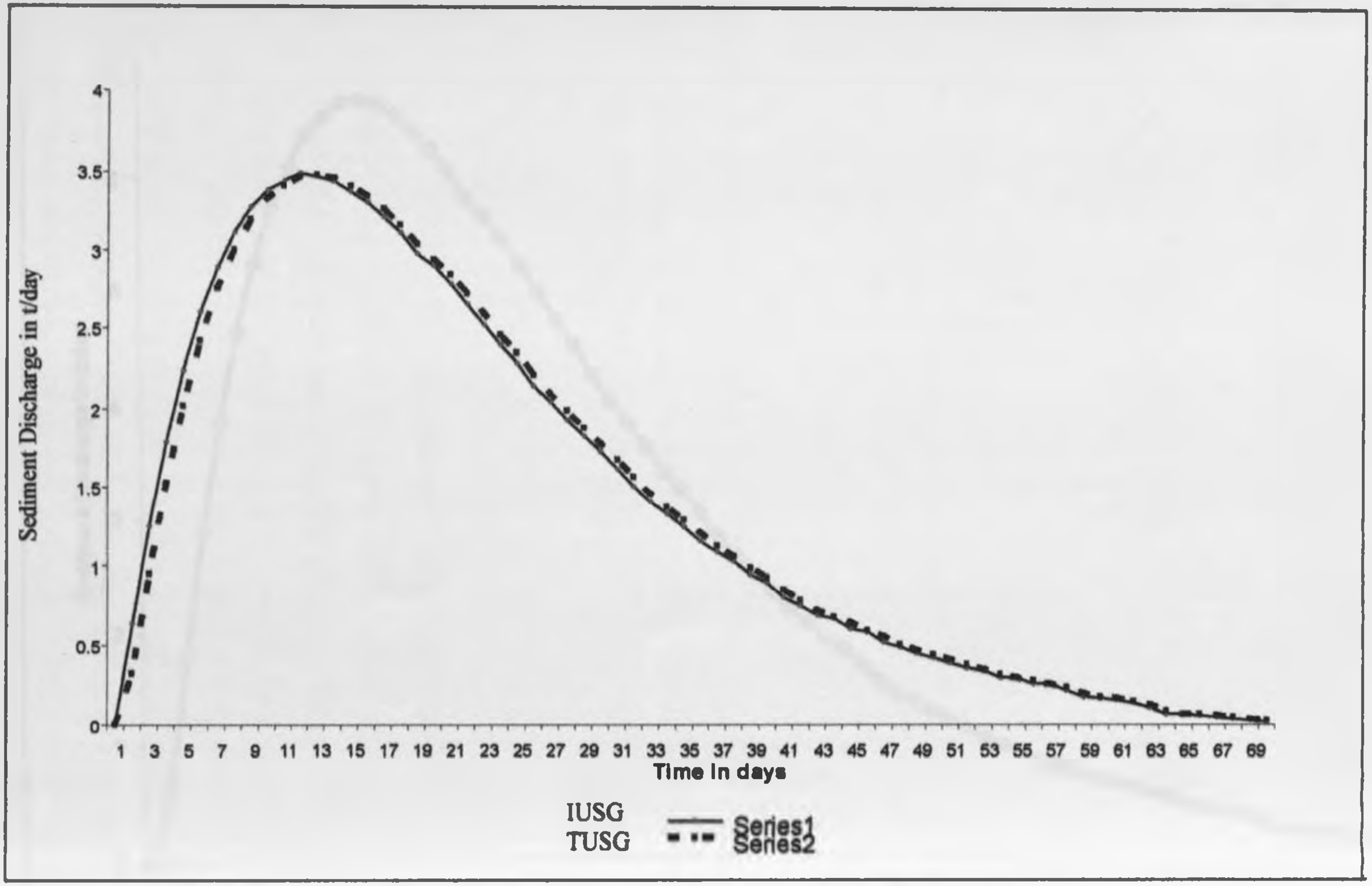

Figure 4.12: Sediment Graph for Both IUSG and TUSG

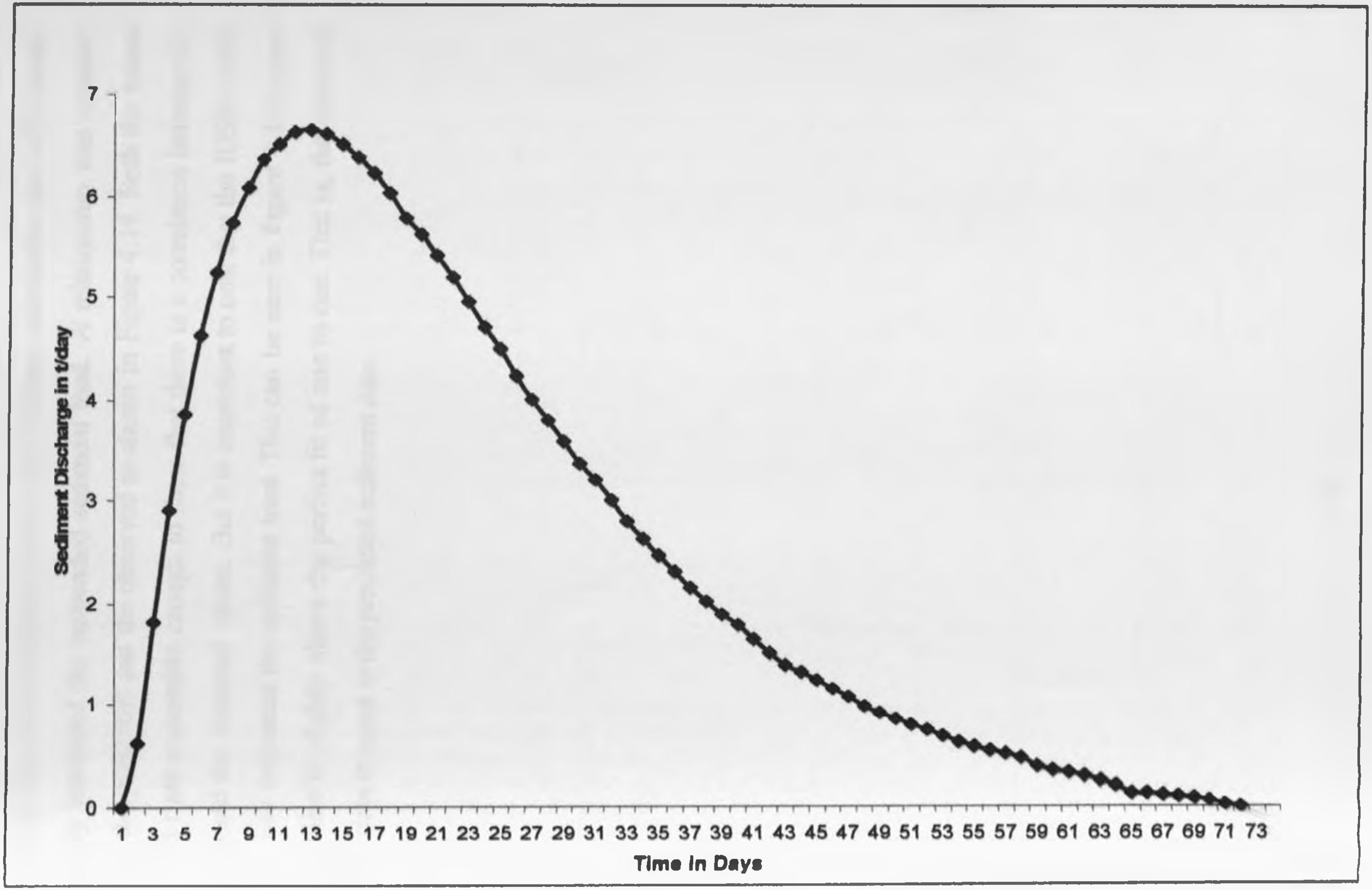

Figure 4.13: The Sub-Catchment Sediment Graph Obtained from the Average Intensity

A comparison of the predicted and the observed sediment data

In Figure 4.14, the predicted sediment data from Figure 4.13 were plotted against the observed values on a log-log plot to aid in finding out whether the IUSG model adequately estimated the suspended sediment load. A relationship was obtained between the predicted and the observed as shown in Figure 4.14. Both the values of R^2 and r are reasonable enough to show that there is a correlation between the predicted and the observed values. But it is important to note that the IUSG model slightly over estimated the sediment load. This can be seen in Figure 4.14, where the fitted line is slightly above the perfect fit of one to one. That is, the observed sediment data is equal to the predicted sediment data.

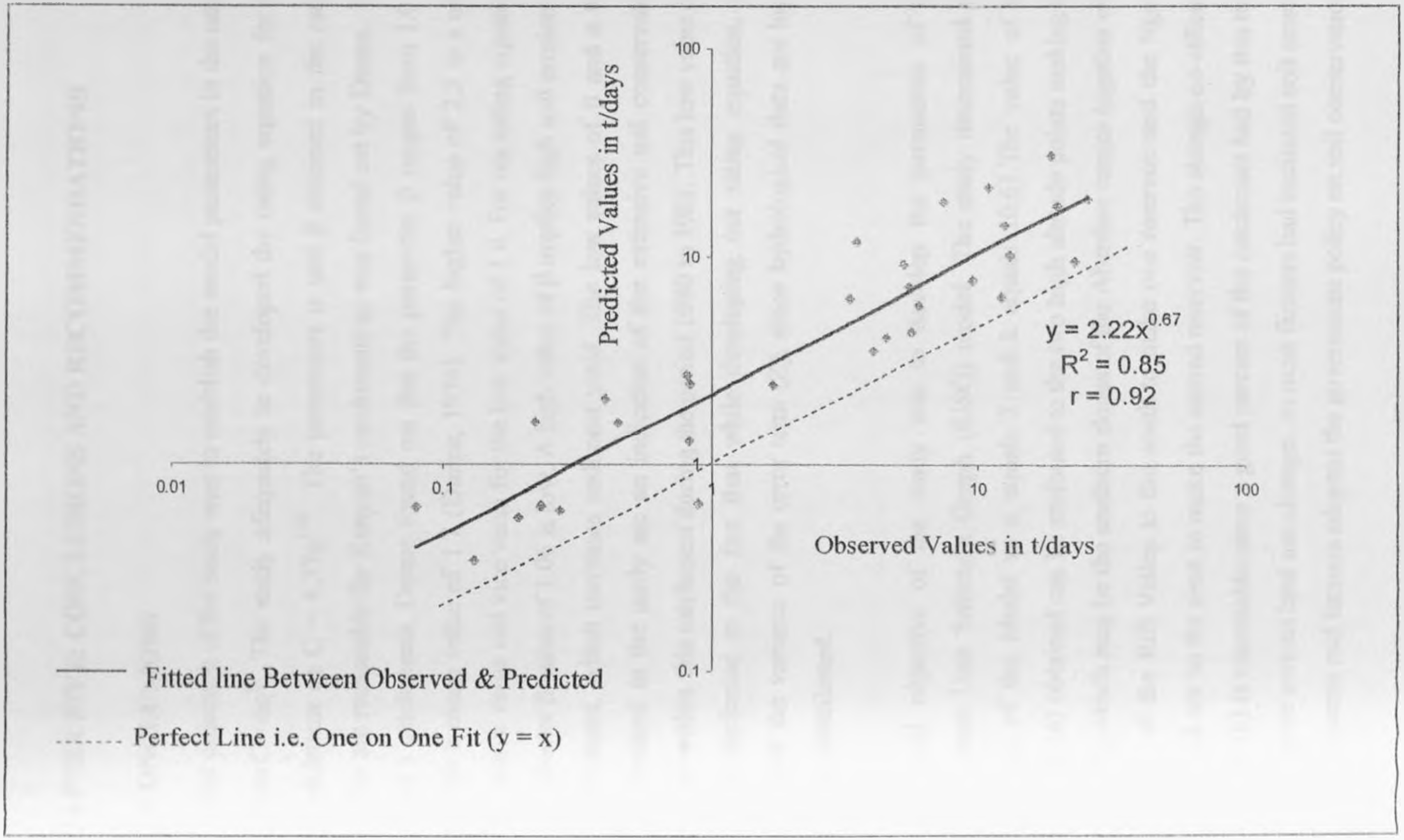

Figure 4.14 : Log-Log Plot of predicted against observed Sediment data

CHAPTER FIVE: CONCLUSIONS AND RECOMMENDATIONS

5.0: CONCLUSIONS

The first objective of the study was to establish the model parameters in the rating equation $C = \alpha q^{\beta}$. The study adequately to developed the rating equation for the sub-catchment as $C = 4.37q^{1.06}$. The parameters α and β obtained in the rating equation are reasonable for Kenyan's catchments as was found out by Dunne. For Kenyan's catchments, Dunne found out that the parameter β ranges from 1.0 to 2.5, with a mean value of 1.7 (Dunne, 1974). The higher value of 2.5 is a non-conservative value and vice versa for the low value of 1.0. For our rating equation, the parameter β value of 1.06 is low. A high value of β implies high soil erosion on the catchment, which increases sediment yield. The low values of β and α that were obtained in the study are an indication of the extensive soil conservation practices within this catchment during the period 1980 to 1981. This low value can also be attributed to the fact that while developing our rating equation, we considered the variance of the error term (Z), since hydrological data are log – normally distributed.

The second objective of the study was to develop the parameters of the Instantaneous Unit Sediment Graph (IUSG) model. The study determined the parameters of the Model as n equals 2 and k equals 10.61.The value of the parameter (n) obtained can be attributed to the two high altitude points making the catchment, which may be the southern slopes of the Aberdare ranges together with the flanks of the Rift Valley to the south to make one reservoir and the Ngong Hills, which are to the west to make the second reservoir. The storage co-efficient parameter (k) is reasonable since a good percent of the catchment had by this time not undergone serious land use changes, as most farmers had instituted soil erosion control measures and farmers adopted the government policy on soil conservation.

The third objective of the study was to simulate the suspended sediment yield from the catchment. The IUSG model based on multi-reservoir cascading concept was able to simulate the yield for the study period as an average of 1.05 million tonnes per year, which is one eighth of the total sediment yield entering the ocean from the whole catchment. The value given by Mansell-Moullin in 1973 was 8.4 million tonnes, when he monitored at the Sabaki River. This gives a sediment production rate of 187.95 t/km^2/yr. This production rate is low and is still within manageable levels compared to rates given by Wain in 1983 as 535 t/km^2/yr for Thwake and 696 t/km^2/yr for Mavindini, all of them in the Athi River catchment.

From this production rate, it is obvious that soil erosion in the catchment is on the increase and may soon exceed the allowable loss. If this situation is not arrested early enough and the catchment used sustainably, then the catchment will no longer be the source of water for towns and the reservoirs may also get filled with sediments. Further consequences might see the Malindi Bay being closed to tourism due to heavy siltation.

5.1 Limitations

Due to lack of resources, the researcher could not be able to gauge the river for the current. It is therefore important to note that the study is based on the data of the 1980s. This limitation implies that the sediment yield simulated does not represent the current sediment yield being generated in the catchment.

Another limitation was that the study could not simulate the total sediment load from the catchment due to lack of data on the bed load component. This difficulty was also faced by Dunne and Wain in their work on the suspended load in Kenya (Dunne, 1974 and Wain, 1983).

5.2 Recommendations

The study was only focused on suspended sediment. Other studies on the catchment by Wain and Dunne were also based on the estimations of the suspended sediments (Dunne, 1974 and Wain, 1983). Therefore, it is recommended that other researchers look into the bed load component, so as to come up with the total sediment yield for the catchment.

The reduction of costs incurred in conventional sediment gauging techniques needs to be addressed. This can be achieved by optimizing the sampling frequency for sediment concentration, using simple sampling equipment and procedures, as well as simplified discharge measuring techniques. The use of Single Velocity Method for discharge measurement has been suggested as a cheap alternative to conventional current meter stream discharge gauging or the use of flow measuring devices. Likewise, grab sampling could be a simple and cost effective means of sampling the suspended sediment, whose potential needs to be investigated. Therefore, it is recommended for our subcatchment that the above methods be employed to enable the researchers give the current status of the sediment yield for the catchment. It is important to note here that the present study is based on the data of the 1980s due to lack of resources to gauge the river for current data. This implies that the results obtained here do not reflect the present sediment yields of the catchment, because many significant changes have taken place since that time.

Sediment yield estimation for the upper Athi-River subcatchment involves a big area (5 590 km^2), and is bound to give inaccurate results. Therefore, it is recommended that the next sediment yield study in the catchment be divided along the main sub-catchments of the Athi River. This will reduce the catchment area to be used in estimating the sediment yield and give more detailed data.

In general it can be noted that the information on non-point pollution has become more important in recent times. This has led to the increase and expansion of study activities on this question. Most developing countries lack the resources for extensive field studies and measurements of non- point pollution and Kenya is no exception. Therefore, it is recommended that there should be an urgent need to formulate evaluation techniques that would be in the cost ability of this country. Use of modeling is in this light recommended but this again calls for the testing and the calibration of the models suggested for use. Also to be investigated in the country is the use of satellite and Radar in obtaining the hydrological data as this will eliminate the laborious process of gauging the catchment for the same.

Another recommendation is the enforcement of the government policies on Soil erosion and sediment control. There should be a law requiring people to put in place soil erosion and sediment control structures and to practice sustainable land use in the catchments. This will ensure continued water supply and land productivity.

REFERENCES

Annadale, G.W., 1987. Reservoir Sedimentation. Elsevier Publication, Amsterdam.

Bartlett, M.S., 1955. Introduction of Stochastic processes. University of Cambridge Press, London.

Bobotti, O.K., 1978. Sediment Monitoring Network and Programme, *Unpublished Report*, Ministry of Water Development, Nairobi, Kenya.

Charania, S.H., 1988. A Strategy for Organising a Sediment Data Collection Network Based on the Available Hydrologic Records for a Catchment in Kenya, Sediment Budgets. *IAHS Publication* No. 174, 181- 188.

Ching, O., P. Smithson. And M. Swallow., 1999. Assessment of Sediment and Nutritional Load in Rivers. *Technical Report on Improved Land Management in the Lake Victoria Basin*. ICRAF. Pg 16 – 17

Chow, V. T., D. R. Maidment. And L .W. Mays. , 1988. Applied Hydrology, McGraw-hill book Company, New York.

Das, G., 2000. Hydrology and Soil Conservation Engineering, Prentice Hall of India, New Delhi.

Das. G. and H.S. Chauhan., 1993. Sediment Routing for Mountainous Himalayan Region, *Trans. ASAE.* 33(1), 95 – 103.

Dendy, F.E. and G.C.Bolton., 1976. Sediment Yield – Runoff – Drainage Area Relationships in the United States. *Journal of soil and water conservation* (31) Pg 264 – 266.

Denga, F.O., G.F.Ongwenyi. and J.U. Kitheka. , 1993. Erosion and Sedimentation Problems in the Arid and Semi-Arid Lands of Kenya. *Proceedings of the 4th National Land and Water Management Workshop*, Nairobi, Kenya.

Dunne, T., 1975. Sediment Yield of Kenyan rivers, Unpublished Report, Ministry of Water Development, Nairobi, Kenya.

Dunne, T. and G.S.Ongweny., 1976. A New Estimate of the Rate of Sediment in Reservoirs on the Upper Tana River. *Kenya Geographical Journal* 2: 109 – 126.

Dunne, T., 1978. Recent and Past Rates of Erosion in Semi Arid Kenya. *Geomorphology Supplement*. 28:91-100.

Dunne, T., 1979. Sediment and Land Use in Tropical Countries. *Journal of Hydrology*. 42: (100-112)

Edward, K.A., 1979. Regional Contrasts in the Rates of Soil Erosion and Their Significant with Respect to Agricultural Development in Kenya. In: Lal.R and Greenland, D.J (Eds). Soil Physical Properties and Crop Production in the Tropics. John Willey and Sons. London. Pg 441 – 454.

Flaxman, E.M., 1972. Predicting Sediment Yield in Western United States. *Journal of Hydraulics Division. ASCE*. PG 2073 – 2085.

Garde, R. J. and V.C. Kootchar. , 1987. Sediment Yields Estimation. *Journal of Irrigation and Power*. India. 44(3): 97-123.

Gikonyo, J.K., 1994. An Instantaneous Sediment Graph Study of Mathare River Catchment.Unpublished MSc Thesis. University of Nairobi, Kenya.

Haan, C.T., 1977. Statistical Methods in Hydrology. The Iowa State University Press, Ames, Iowa, USA.

Linsley, R.K , R. K. Kholer and J. H. Paulhas., 1988. Hydrology for Engineers. Mc-Graw Hill Book Company (International Edition).

Kinori, B.Z. and J. Mevorach. , 1984. Manual of Surface Drainage in Engineering. Vol.2. (Stream Flow Engineering and Flood Protection), Elsevier Publication. Amsterdam.

Kumar, S. and R.A. Rastogi. , 1987. A Conceptual Catchment Model for Estimation of Suspended Sediment Flow. *Journal of Hydrology*. 95:155-163.

Mansell – Moullin, M., 1973. Report on the Hydrology of the Sabaki River. Report to Kenya Government, Ministry of Water Development.

Nash, J.E., 1957. The form of Instantaneous Unit Hydrograph. *IASH Publication*, No.45,Page 114 – 121.

Nordin, C.F., 1991. Sediment Problems. *International Journal of Sediment Research*. Vol. 6: 11 – 17.

Olwero, J.G.N., 1997. Some Aspects of Drought in the Lake Victoria Catchment. MSc Thesis, University of Nairobi.

Ongweny, G.S., 1978. Erosion and Sediment Transport in the Upper Tana Catchment with Special Reference to the Thiba Basin, Ph.D. Thesis, University of Nairobi, Kenya.

Opere, A.O., 1991. The Use of a Rainfall – Runoff Model in the Forecasting of Discharge from Rainfall in the Upper Athi River Catchment. MSc Thesis, University of Nairobi.

Ranga Raju, K.G, and R.J. Garde., 1985. Mechanics of Sediment Transportation and Alluvial Stream Problems. Wiley Eastern, New Delhi. India.

Rendon-Herrero, O., 1975. Estimation of Wash Load Produced on Certain Small Watersheds. *Journal of Hydraulics Division* ASAE.100: 838-848.

Singh, V. P. and V.J. Chen. , 1982. An Instantaneous Unit Sediment Graph Study for Small Upland Watershed. Water Resources Publication. Colorado, U.S.A.

Singh, V.P. and P.F.Krostanovic. , 1987. A Stochastic Model for Sediment Yields Using the Principle of Maximum Entropy. *Water Resources Research*. 23(5): 781-793.

Sharma, T.C. and W.T. Dickinson., 1979. Discrete Dynamic Model of Watershed Sediment Yield. *Journal of Hydraulics Division*. ASCE. 105: 535-571.

Sharma, T.C. and W.T. Dickinson., 1980. System Model of Daily Sediment Yield. *Water Resources Research*, 16(3) Pg 501 – 506.

Sharma, T.C., 1993. Some Conceptions of the Sediment Rating Equations. *Proceedings of the 4th National Land and Water Management Workshop.* Nairobi, Kenya.

Sharma, T.C., 1994. Erosion and Sedimentation. Unpublished *MSc Lecture Notes*. Department of Agricultural Engineering. University of Nairobi.

Sharma, T.C., 1999. Advanced Applied Hydrology. *Unpublished Lecture Notes.* School of Environmental Studies. Moi University. Eldoret, Kenya.

Shaw, E.L 1988. Hydrology in Practice. Chapman and Hall (Third Edition).

Sutherland, R.A. and R.B.Bryan., 1986. Sediment Budget Studies in the Katiorin Catchment, Baringo: A Preliminary Report in the Soil and Water Conservation in Kenya, *Proceedings of the Third National Soil Conservation Workshop*, Kabete, Kenya. Pg 88 – 98.

Suresh, R., 1997. Soil and Water Conservation Engineering. Standard Publishers Distributors. Delhi, India.

TARDA 1981. Athi River Basin Pre-investment Study. Annexes 1-2.Tana and Athi River Development Authority. Nairobi, Kenya.

Thomas, D.J. and K.A. Edwards. , 1979. Runoff, Erosion and Conservation in a Representative Basin in Machakos District, Kenya. Proceedings of an *International Conference on Agricultural Hydrology and Watershed Management*, Ibadan, Nigeria.

Thomas, D. B., K.A. Edwards. , R.G. Barber. and I.G.G. Hogg. , 1981. Runoff, Erosion and Conservation in a Representative Basin in Machakos district, Kenya. In: Lal.R and Russell, E.W. (eds). Tropical Agricultural Hydrology, John Willey and Sons. London. Pg 395 – 417.

Vansickle, J. and R.L. Beschta. , 1983. Supply Based Model of Suspended Sediment Transport in Streams. *Water Resources Research Vol.* 19:768-778.

Wain, A.S., 1983. Athi River Sediment Yield and the Significant of Water Resources Development. Soil and Water Conservation in Kenya. *IDS Occasional Paper No. 42.* University of Nairobi, Kenya.

Williams, J.R., 1975. Sediment Yield Prediction with Universal Equation Using Runoff Energy Factor. *USDA Publication* No.40: 244-252.

Williams, J. R., 1978. A Sediment Graph Model Based on an Instantaneous Unit Sediment Graph. *Water Resources Research*. 14(4): 659-664.

Wischmeier, W.H., and D.D. Smith., 1958. Rainfall Energy and its Relationship to Soil Loss, *Trns. AM. Geophy. Union*, (39): 285-291.

Zachar, D.C., 1982. Soil Erosion. Elservier Scientific Publishing Company. Amsterdam.

Appendix 1: Derivation of Nash Gamma Function form of IUH

The IUH is the outflow hydrograph from a cascade of n linear reservoirs subjected to unit impulse input applied during the infinitesimal time interval of δT such that δT tends to 0. In other words the unit impulse is input to the first linear reservoir and the resulting outflow is the IUH of the single linear reservoir system. That is,

$$q(t) = \int_0^t U(t-\tau).I(\tau)\partial\tau = U(t); \text{where} I(\tau)=1, \text{for } \tau=0 \quad \text{and } I(\tau)=0 \text{ for } \tau>0.$$

For a linear reservoir under the condition of instantaneous input, i.e. at t=0

$$S = 1 \text{ hence } q(0) = 1/k.$$

For t>0, the equation of continuity can be written as

$$I - q = \frac{ds}{dt} = k\frac{dq}{dt} \quad \text{Thus}$$

$$\frac{dq}{dt} + \frac{1}{k}q = 0, \text{ since I=0 for } t > 0$$

The solution of the above differential equation is,

$$q(t) = c_o e^{\frac{-t}{k}} \quad \text{Where } c_o \text{ is the constant of integration}$$

When,

$$t = 0; q = \frac{1}{k} \text{ hence } c_0 = \frac{1}{k}, \text{ therefore}$$

$$q(t) = \frac{1}{k}e^{\frac{-t}{k}} = u(t)$$

It can be illustrated diagrammatically as

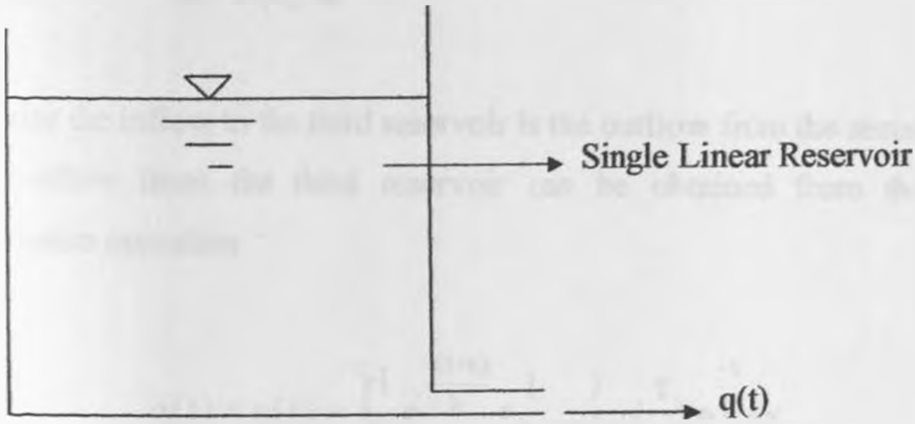

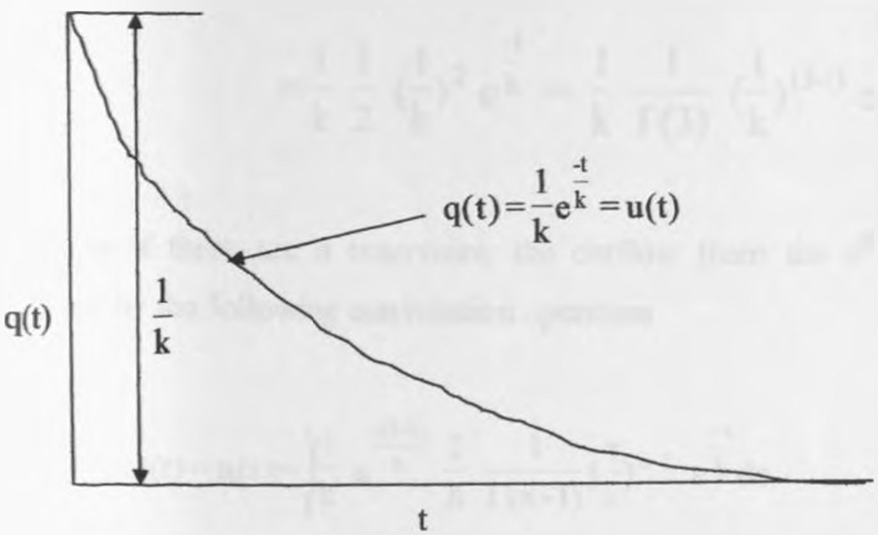

The above q (t) is the input to the second linear reservoir hence the output from the second reservoir can be obtained from the following convolution integral

$$q(t)=\int_0^t u(t-\tau).\frac{1}{k}e^{\frac{-\tau}{k}}d\tau \quad = \quad \int_0^t \frac{1}{k}e^{\frac{-(t-\tau)}{k}}.\frac{1}{k}e^{\frac{-\tau}{k}}d\tau$$

$$= \frac{1}{k}\left(\frac{t}{k}\right)e^{\frac{-t}{k}} = \frac{1}{k}\bullet\frac{1}{\Gamma(2)}\left(\frac{t}{k}\right)^{(2-1)}e^{\frac{-t}{k}} = u(t)$$

Likewise the inflow to the third reservoir is the outflow from the second reservoir. The outflow from the third reservoir can be obtained from the following convolution operation.

$$q(t)=u(t)=\int_0^t \frac{1}{k}e^{\frac{-(t-\tau)}{k}} \bullet \frac{1}{k}\cdot\frac{1}{\Gamma(2)}\left(\frac{\tau}{k}\right)e^{\frac{-\tau}{k}}d\tau$$

$$=\frac{1}{k}\,\frac{1}{2}\,\left(\frac{t}{k}\right)^2 e^{\frac{-t}{k}} = \frac{1}{k}\,\frac{1}{\Gamma(3)}\,\left(\frac{t}{k}\right)^{(3-1)}e^{\frac{-t}{k}}$$

Likewise if there are n reservoirs, the outflow from the n^{th} reservoir can be obtained by the following convolution operation

$$q(t)=u(t)=\int_0^t \frac{1}{k}\,e^{\frac{-(t-\tau)}{k}}\,\frac{1}{k}\,\frac{1}{\Gamma(n-1)}\left(\frac{\tau}{k}\right)^{n-2}\,e^{\frac{-\tau}{k}}d\tau$$

$$q(t)=U(t)=\frac{1}{k\Gamma n}\,\left(\frac{t}{k}\right)^{n-1}e^{\frac{-t}{k}}$$

Where

U (t) = ordinates of the IUSG (tones/hr).

n = number of routing reservoirs.

k = storage constant of the reservoirs (hr).

The above expression for IUH is analogous to the gamma probability function with the parameters n and k. In normal course most of the natural catchments can be modeled with n = 2 or 3 (Shaw, 1988).

Appendix 2: Table 4.7: The ordinates of the IUH and IUSG Model Developed

Time in Days	$\frac{1}{k\Gamma n}$	$e^{-\frac{t}{k}}$	$\left(\frac{t}{k}\right)^{n-1}$	U (t) m^3/hr	IUH U (t) m^3/day	IUSG t/day
0	0.091	1	0	0	0	0
1	0.091	0.910	0.082	0.00679	0.163	0.64
2	0.091	0.829	0.170	0.013	0.308	1.25
3	0.091	0.754	0.261	0.018	0.430	1.79
4	0.091	0.687	0.355	0.022	0.533	2.24
5	0.091	0.625	0.449	0.026	0.613	2.60
6	0.091	0.569	0.545	0.028	0.677	2.89
7	0.091	0.518	0.642	0.030	0.726	3.11
8	0.091	0.471	0.739	0.032	0.760	3.27
9	0.091	0.429	0.837	0.033	0.784	3.38
10	0.091	0.391	0.936	0.033	0.799	3.44
11	0.091	0.356	1.04	0.033	0.809	3.49
12	0.091	0.324	1.136	0.033	0.804	3.47
13	0.091	0.295	1.237	0.033	0.797	3.44
14	0.091	0.268	1.338	0.033	0.783	3.37
15	0.091	0.244	1.439	0.032	0.767	3.30
16	0.091	0.222	1.541	0.031	0.747	3.21
17	0.091	0.202	1.643	0.030	0.725	3.11
18	0.091	0.184	1.746	0.029	0.696	2.98
19	0.091	0.168	1.849	0.028	0.678	2.89
20	0.091	0.153	1.952	0.027	0.652	2.78
21	0.091	0.139	2.056	0.026	0.624	2.65
22	0.091	0.126	2.160	0.025	0.569	2.52

Time in Days	$\frac{1}{k\Gamma n}$	$e^{-\frac{t}{k}}$	$\left(\frac{t}{k}\right)^{n-1}$	U (t) m^3/hr	IUH U (t) m^3/day	IUSG t/day
23	0.091	0.115	2.264	0.024	0.569	2.40
24	0.091	0.105	2.368	0.023	0.543	2.29
25	0.091	0.095	2.473	0.021	0,513	2.15
26	0.091	0.087	2.578	0.020	0.490	2.05
27	0.091	0.079	2.683	0.019	0.463	1.93
28	0.091	0.072	2.789	0.018	0.439	1.83
29	0.091	0.066	2.895	0.017	0.417	1.73
30	0.091	0.060	3.000	0.016	0.393	1.62
31	0.091	0.054	3.107	0.015	0.366	1.51
32	0.091	0.049	3.213	0.014	0.344	1.41
33	0.091	0.045	3.319	0.014	0.326	1.33
34	0.091	0.041	3.426	0.013	0.307	1.25
35	0.091	0.037	3.533	0.012	0.285	1.16
36	0.091	0.034	3.640	0.011	0.270	1.09
37	0.091	0.031	3.747	0.011	0.254	1.02
38	0.091	0.028	3.855	0.0098	0.236	0.95
39	0.091	0.026	3.963	0.0093	0.225	0.90
40	0.091	0.023	4.070	0.0085	0.204	0.81
41	0.091	0.021	4.178	0.0080	0.192	0.76
42	0.091	0.019	4.286	0.0074	0.178	0.70
43	0.091	0.018	4.395	0.007	0.173	0.68
44	0.091	0.016	4.503	0.0065	0.157	0.61
45	0.091	0.015	4.612	0.0062	0.151	0.59
46	0.091	0.013	4.720	0.0055	0.134	0.52
47	0.091	0.012	4.829	0.0052	0.127	0.49
48	0.091	0.011	4.938	0.0050	0.116	0.45

Time in Days	$\frac{1}{k\Gamma n}$	$e^{-\frac{t}{k}}$	$\left(\frac{t}{k}\right)^{n-1}$	U (t) m^3/hr	IUH U (t) m^3/day	IUSG t/day
49	0.091	0.010	5.047	0.0045	0.110	0.42
50	0.091	0.009	5.156	0.004	0.102	0.39
51	0.091	0.0083	5.266	0.004	0.095	0.36
52	0.091	0.0075	5.375	0.004	0.09	0.34
53	0.091	0.0069	5.485	0.003	0.08	0.3
54	0.091	0.0063	5.595	0.003	0.08	0.3
55	0.091	0.0057	5.705	0.003	0.07	0.26
56	0.091	0.0052	5.815	0.003	0.07	0.26
57	0.091	0.0047	5.925	0.003	0.06	0.22
58	0.091	0.0043	6.035	0.002	0.05	0.18
59	0.091	0.0039	6.145	0.002	0.05	0.17
60	0.091	0.0036	6.258	0.002	0.04	0.16
61	0.091	0.0032	6.366	0.002	0.04	0.14
62	0.091	0.0029	6.477	0.002	0.03	0.11
63	0.091	0.0027	6.588	0.002	0.02	0.07
64	0.091	0.0024	6.699	0.001	0.02	0.07
65	0.091	0.0022	6.810	0.001	0.02	0.06
66	0.091	0.0020	6.921	0.001	0.02	0.05
67	0.091	0.0018	7.032	0.001	0.02	0.04
68	0.091	0.0017	7.143	0.001	0.01	0.03
69	0.091	0.0015	7.255	0.001	0.01	0.02
70	0.091	0.0013	7.366	0.0009	0.01	0.001

Appendix 3: Gamma Function

n	Γn	n	Γn
1	1.000000	1.52	0.887039
1.02	0.988844	1.54	0.888178
1.04	0.978438	1.56	0.889639
1.06	0.968744	1.58	0.891420
1.08	0.959725	1.60	0.893515
1.10	0.951351	1.62	0.895924
1.12	0.943590	1.64	0.898642
1.14	0.936416	1.66	0.901668
1.16	0.929803	1.68	0.905001
1.18	0.923728	1.70	0.908639
1.20	0.918169	1.72	0.912581
1.22	0.913106	1.74	0.916826
1.24	0.908521	1.76	0.921375
1.26	0.904397	1.78	0.926227
1.28	0.900718	1.80	0.931384
1.30	0.897471	1.82	0.936845
1.32	0.894640	1.84	0.942612
1.34	0.892216	1.86	0.948687
1.36	0.890185	1.88	0.955071
1.38	0.888537	1.90	0.961766
1.40	0.887264	1.92	0.968774
1.42	0.886356	1.94	0.976099
1.44	0.885805	1.96	0.983743
1.46	0.885604	1.98	0.991708
1.48	0.885747	2.00	1.000000

1.50	0.886227		

Appendix 4: Suspended Sediment and Water Discharge Data

STATION CODE	RIVER NAME	SAMPLING DATES	WATER LEVEL (CM)	WATER DISCHARGE M^3/S	SUSPENDED LOAD (PPM)
3DA02	ATHI	18-01-1980	50	3	7
3DA02	ATHI	04-03-1980	45	4	9
3DA02	ATHI	08-04-1980	44	4	15
3DA02	ATHI	10-04-1980	40	3	18
3DA02	ATHI	11-04-1980	47	5	15
3DA02	ATHI	12-04-1980	55	5	18
3DA02	ATHI	13-04-1980	50	6	12
3DA02	ATHI	14-04-1980	48	4	16
3DA02	ATHI	15-04-1980	56	5	22
3DA02	ATHI	16-04-1980	65	7	33
3DA02	ATHI	17-04-1980	66	9	25
3DA02	ATHI	18-04-1980	65	7	42
3DA02	ATHI	19-04-1980	70	10	98
3DA02	ATHI	19-04-1980	80	11	84
3DA02	ATHI	20-04-1980	107	20	133
3DA02	ATHI	21-04-1980	97	16	607
3DA02	ATHI	21-04-1980	92	14	232
3DA02	ATHI	24-04-1980	99	20	246

STATION CODE	RIVER NAME	SAMPLING DATES	WATER LEVEL (CM)	WATER DISCHARGE M^3/S	SUSPENDED LOAD (PPM)
3DA02	ATHI	02-05-1980	56	6	41
3DA02	ATHI	03-05-1980	189	43	1292
3DA02	ATHI	03-05-1980	177	53	278
3DA02	ATHI	04-05-1980	236	64	862
3DA02	ATHI	04-05-1980	258	99	811
3DA02	ATHI	06-05-1980	214	69	679
3DA02	ATHI	07-05-1980	377	190	1050
3DA02	ATHI	07-05-1980	365	167	1033
3DA02	ATHI	08-05-1980	335	170	632
3DA02	ATHI	09-05-1980	408	231	349
3DA02	ATHI	10-05-1980	194	70	525
3DA02	ATHI	12-05-1980	235	100	521
3DA02	ATHI	14-05-1980	307	161	1163
3DA02	ATHI	17-05-1980	206	81	424
3DA02	ATHI	27-05-1980	139	40	174
3DA02	ATHI	28-05-1980	133	36	198
3DA02	ATHI	31-05-1980	256	124	800
3DA02	ATHI	01-06-1980	240	111	520
3DA02	ATHI	02-06-1980	174	63	221
3DA02	ATHI	04-06-1980	140	43	113

STATION CODE	RIVER NAME	SAMPLING DATES	WATER LEVEL (CM)	WATER DISCHARGE M^3/S	SUSPENDED LOAD (PPM)
3DA02	ATHI	05-06-1980	184	39	121
3DA02	ATHI	19-06-1980	106	3	81
3DA02	ATHI	21-07-1980	80	12	139
3DA02	ATHI	15-09-1980	57	5	86
3DA02	ATHI	30-09-1980	52	4	50
3DA02	ATHI	24-10-1980	49	4	53
3DA02	ATHI	10-11-1980	98	19	139
3DA02	ATHI	13-11-1980	82	14	85
3DA02	ATHI	17-11-1980	209	74	640
3DA02	ATHI	13-12-1980	47	4	44
3DA02	ATHI	24-02-1981	47	3	0
3DA02	ATHI	12-03-1981	42	2	0
3DA02	ATHI	31-03-1981	103	20	0
3DA02	ATHI	03-04-1981	214	83	1
3DA02	ATHI	04-04-1981	183	65	1
3DA02	ATHI	06-04-1981	270	118	3
3DA02	ATHI	06-04-1981	263	114	2
3DA02	ATHI	07-04-1981	358	220	9
3DA02	ATHI	08-04-1981	136	36	0
3DA02	ATHI	09-04-1981	107	24	1

STATION CODE	RIVER NAME	SAMPLING DATES	WATER LEVEL (CM)	WATER DISCHARGE M^3/S	SUSPENDED LOAD (PPM)
3DA02	ATHI	13-04-1981	686	715	5
3DA02	ATHI	15-04-1981	262	124	1
3DA02	ATHI	15-04-1981	251	118	1
3DA02	ATHI	16-04-1981	287	141	1
3DA02	ATHI	16-04-1981	270	135	1
3DA02	ATHI	18-04-1981	386	227	1
3DA02	ATHI	22-04-1981	183	69	0
3DA02	ATHI	08-05-1981	221	93	1
3DA02	ATHI	09-05-1981	357	221	2
3DA02	ATHI	10-05-1981	555	495	1
3DA02	ATHI	11-05-1981	251	120	1
3DA02	ATHI	15-05-1981	670	677	2
3DA02	ATHI	16-05-1981	472	328	1
3DA02	ATHI	16-05-1981	544	371	1
3DA02	ATHI	19-05-1981	296	154	0
3DA02	ATHI	22-05-1981	121	276	0
3DA02	ATHI	06-07-1981	106	23	0
3DA02	ATHI	20-07-1981	103	22	89
3DA02	ATHI	17-08-1981	83	14	76
3DA02	ATHI	14-09-1981	72	11	31

STATION CODE	RIVER NAME	SAMPLING DATES	WATER LEVEL (CM)	WATER DISCHARGE M^3/S	SUSPENDED LOAD (PPM)
3DA02	ATHI	12-10-1981	62	6	92
3DA02	ATHI	14-11-1981	64	8	79
3DA02	ATHI	19-11-1981	71	9	64
3DA02	ATHI	04-01-1981	56	6	49
3DA02	ATHI	01-02-1981	41	3	24
3DA02	ATHI	01-03-1982	34	2	25